



Article

Quantum Mechanics and Control Using Fractional Calculus: A Study of the Shutter Problem for Fractional Quantum Fields

Jonathan Blackledge ^{1,2,3,4,5,†}

- ¹ Science Foundation Ireland, Three Park Place, Hatch Street Upper, Saint Kevin's, D02 FX65 Dublin, Ireland; jonathan.blackledge@tudublin.ie; Tel.: +44-7584-676960
- ² Centre for Advanced Studies, Warsaw University of Technology, Plac Politechniki 1, 00-661 Warsaw, Poland
- ³ Department of Computer Science, University of Western Cape, Robert Sobukwe Road, Bellville, Cape Town 7535, South Africa
- ⁴ Faculty of Arts, Science and Technology, Wrexham Glyndŵr University of Wales, Mold Road, Wrexham LL11 2AW, UK
- ⁵ School of Mathematics, Statistics and Computer Science, University of KwaZulu-Natal, University Road, Westville, Durban 3629, South Africa
- † Current address: School of Electrical and Electronic Engineering, Technological University Dublin, Grangegorman, D07 EWW4 Dublin, Ireland.

Abstract: The 'diffraction in space' and the 'diffraction in time' phenomena are considered in regard to a continuously open, and a closed shutter that is opened at an instant in time, respectively. The purpose of this is to provide a background to the principal theme of this article, which is to extend the 'quantum shutter problem' for the case when the wave function is determined by the fundamental solution to a partial differential equation with a fractional derivative of space or of time. This involves the development of Green's function solutions for the space- and time-fractional Schrödinger equation and the time-fractional Klein–Gordon equation (for the semi-relativistic case). In each case, the focus is on the development of primarily one-dimensional solutions, subject to an initial condition which controls the dynamical behaviour of the wave function. Coupled with variations in the fractional order of the fractional derivatives, illustrative example results are provided that are based on presenting space-time maps of the wave function; specifically, the probability density of the wave function. In this context, the paper provides a case study of fractional quantum mechanics and control using fractional calculus.

Keywords: fractional quantum mechanics; quantum shutter problem; diffraction in time; fractional diffusion equation; fractional Schrödinger equation; fractional Klein–Gordon equation



Citation: Blackledge, J. Quantum Mechanics and Control Using Fractional Calculus: A Study of the Shutter Problem for Fractional Quantum Fields. *Appl. Mech.* **2022**, *3*, 413–463. <https://doi.org/10.3390/applmech3020026>

Received: 7 February 2022

Accepted: 16 March 2022

Published: 12 April 2022

Publisher's Note: MDPI stays neutral with regard to jurisdictional claims in published maps and institutional affiliations.



Copyright: © 2022 by the author. Licensee MDPI, Basel, Switzerland. This article is an open access article distributed under the terms and conditions of the Creative Commons Attribution (CC BY) license (<https://creativecommons.org/licenses/by/4.0/>).

1. Introduction

In 1952, Marcos Moshinsky published a seminal article entitled 'Transient Phenomena in Quantum Mechanics: Diffraction in Time' [1]. Using a one-dimensional model, Moshinsky considered the case when a beam of non-relativistic electrons (travelling from left to right in the negative half-space) is incident upon a shutter (placed at $x = 0$) so that they cannot propagate through to the positive half-space. At a time $t = 0$, the shutter is opened instantaneously so that the electron beam can propagate through from the negative to the positive half-space. The problem is to evaluate the probability density of the resulting wave-function (determined by the Schrödinger equation) in the positive half-space as a function of both space and time. In other words, if $u(x, t)$ is taken to be the electron wave-field, then what is the (x, t) map, for $x > 0$ and $t > 0$ of $|u(x, t)|^2$ when the shutter is opened at $t = 0$?

The space-time characteristics of the probability density are governed by the initial condition $u_0(x) \equiv u(x, 0)$ of the field at $t = 0$, where $u_0(x)$ is taken to represent of the electron beam in the negative half-space. In this context, the study undertaken by

Moshinsky was an example of a control problem in quantum mechanics. The analysis undertaken by him involved developing a Green's function solution to the homogeneous time-dependent Schrödinger equation [2]. For atomic units (where the Dirac constant and the electron mass are set to 1), this equation is identical to the homogeneous time-dependent diffusion equation for a Diffusivity of $1/2$ but with imaginary time. Consequently, the Green's function for the time-dependent diffusion equation (for a Diffusivity of $1/2$), which includes the function $\exp(-x^2/2t)$, yields a solution to the Schrödinger equation, which is characterised by the function $\exp(ix^2/2t)$.

For a fixed value of t , this is a 'chirp function' of space (a linear frequency modulated chirp with a 'chirp parameter' of $1/2t$). It is therefore analogous to the convolution kernel associated with Fresnel diffraction [3] which is characterised by a quadratic phase factor [4]. However, for a fixed value of x , as $t \rightarrow 0$, the function $\exp(-x^2/2t)$ oscillates at an increasingly high frequency, characterised by an inverse phase factor of time. For this reason, the phenomenon has been referred to as 'Diffraction in Time' (or even 'Time Scattering') [5,6]. The principal point here is that, unlike the diffusion equation, the same Green's function solution applied to the Schrödinger equation yields a fundamentally different result, which is compounded in the oscillations of the wave-field in space but also, and, more significantly, in time.

The exact nature of these Fresnel-type oscillations depends on the initial condition, but the fact that such oscillations in time occur at all is due entirely to the characteristics of the Green's function alone. This result illustrates a fundamental physical phenomenon, namely that a stream of electrons described by a plane wave-function with a fixed frequency, will spontaneously undergo rapid oscillations in time as soon as the shutter is opened. While such oscillations decrease in frequency (and amplitude) over time, the result shows that the electron wave-field spontaneously oscillates, due to the instantaneous opening of the shutter alone (with no other physical interactions). Such a transient phenomenon is now recognised as being a ubiquitous phenomenon in quantum dynamics [7,8], and, some fifty years after Moshinsky proposed such a dynamic process on theoretical grounds alone, experimental confirmation of the phenomenon was provided in 1996 using ultra-cold atoms [9].

The experimental verification of the 'Quantum Shutter Problem', as it has come to be known, has led to a number of publications which have looked into the evaluation of the problem in three dimensions [10], general formulations [11], new theories of diffraction in time [12], and an extension of the problem to include relativistic effects for both spin-less and half-spin particle beams [13].

There are numerous applications to which fractional calculus is becoming a central theme [14]. In this respect, its application to quantum mechanics has and continues to be explored. Many relatively recent publications (e.g., [15–17]) are paving the way for a future study of fractal geometry in quantum mechanics, for example, using fractional calculus. In this context, the material reported in this paper belongs to the same field of study. It is focusing on the quantum shutter problem and extends it further to include a study of the following:

- a solution to the one-dimensional space-fractional Schrödinger equation;
- a solution to the one-dimensional time-fractional Schrödinger equation;
- a solution to the one-dimensional time-fractional Klein–Gordon equation.

A schematic diagram, which is referred to throughout the paper, is given in Figure 1. Known generically as the 'shutter problem', in this paper, we consider the diffraction-type patterns that occur when a fractional partial differential equation is taken to govern the quantum field that is generated.

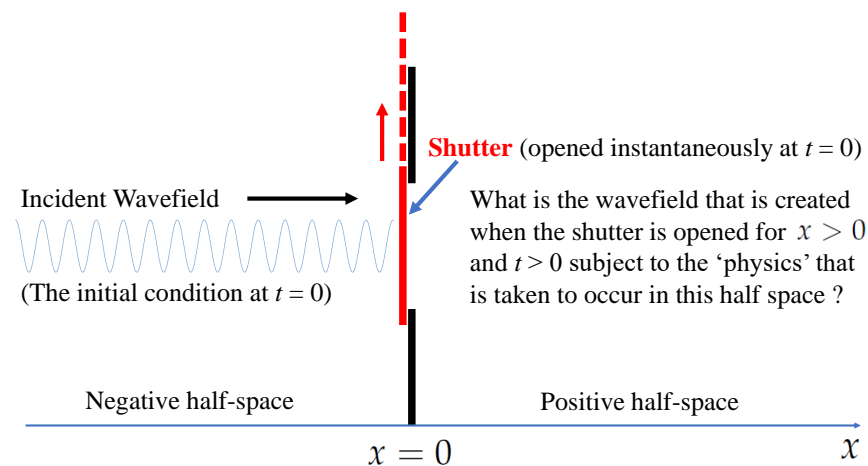


Figure 1. Schematic diagram of the shutter problem for which the following question is relevant: What is the wave-field generated in the positive half-space when the shutter is opened instantaneously at $t = 0$, subject to the ‘physics’ (quantified by the partial differential equation which defines the physical model) that is taken to occur?

1.1. Focus and Context

The principal purpose of this paper is the study of a control problem associated with the scattering and the transient behaviour of a quantum field described by a fractional differential equation. This is an extension to the quantum shutter problem. However, in order to provide a more general and informative context, the paper includes a study of scattering theory for both an Electromagnetic (EM) and a Quantum Mechanical (QM) field. This is done in order to place the quantum shutter problem in a framework that attempts to show the connectivity between the scattering of EM and QM fields and their diffraction from:

- (i) a shutter that is permanently open and produces a diffraction pattern that is a function of space alone and independent of time;
- (ii) a shutter is opened at an instant in time and produces a diffraction-type pattern that is a function of both space and time.

By providing a review of the mathematical models associated with points (i) and (ii) above, the paper provides the reader with the background to the focus for this work and the original contributions that are developed. This is specifically concerned with an investigation of point (ii) for a fractional case, which is an example of quantum mechanics and control using Fractional Calculus. In this case, we are concerned with the control of a fractional QM field that is determined by the initial condition(s) that are applied.

In order to develop the themes presented in this paper in a way that is dimensionally compatible with the original QM shutter problem (where a time-dependent solution is developed for a one-dimensional space), the time-independent analysis is presented for the two-dimensional domain. In this way, for the time-independent problem, solutions are sought for $\mathbf{r} \in \mathbb{R}^2$ and presented graphically in the (x, y) -plane.

With regard to the time-dependent problem, solutions are evolved for $\mathbf{r} \in \mathbb{R}^1$ and presented graphically (as colour-coded maps) in the (x, t) -plane. There is no attempt to provide any specific quantitative measures of the solutions. Rather, the emphasis is to investigate the field patterns that occur for the different models that are investigated coupled with different example parameter values.

A complementary reason for taking this approach is that a two-dimensional time-independent scattering theory is relatively less well documented and reported on than is the three-dimensional case. The material provided therefore fills a gap in the literature as well as providing an informative way of comparing solutions in the (x, y) -plane (time-independent model) and the (x, t) -plane (time-dependent model).

In this way, the paper provides a review of some of the principle methods for investigating the scattering of EM and QM fields for both the time-independent and time-dependent cases. In doing so, it provides the necessary background for an exploration of the space- and time-scattering of QM fields in a unified context. This allows the reader to comprehend the differences, but, primarily, the similarities in the development of the models introduced and the solutions thereof, which are, in the latter case, primarily dependent on the characteristics of the time-independent or time-dependent Green's functions [2].

1.2. Structure and Organisation

Section 2 provides the essential mathematical preliminaries that are used throughout the paper. This includes the definitions used, notation, and a list of important Fourier and Laplace transform relationships, for example. In Section 3, a short overview is given on the fundamental solutions to fractional partial differential equations, introducing the issues associated with how to define a fractional differential of a spatial and temporal function. This includes the use of the Mittag-Leffler function for solving initial value problems [18]. The function is fundamental in developing solutions to applications that involve partial differential equations of fractional order. This is briefly discussed in Section 3, which introduces the role that the Mittag-Leffler plays in a Laplace (and Fourier) transform approach to solving the time fractional diffusion equation, to yield a fundamental solution [19].

Section 4 is designed to provide a short review of classical diffraction theory for scalar EM and QM fields. The purpose of this section is to quantify the principles of scattering theory, and, in doing so, explain the theory of diffraction from an aperture in terms of the far- and intermediate-fields. In the latter case, it is shown why the field pattern is determined by a Fresnel kernel (a complex exponential with a quadratic phase factor) which provides a crucial connectivity with the quantum shutter problem. This is undertaken in Section 5.

In regard to the shutter problem, and, in order to put it into a more general context, Section 6 considers the equivalent problem for a EM field. This leads to a pivotal issue in the flow of the material when, in Section 7, we consider how to model multiple scattering events in terms of a random walk process. In this respect, we consider the case when the shutter is open, but instead of the field propagating through the aperture and evolving in a homogenous positive half-space, the space is taken to be composed of a complex of random distributed scatterers, each with a spatial size that is of the same order as the wavelength of either an EM and QM field.

Coupled with the introduction of a new and exact scattering solution to this problem, multiple scattering effects are modelled in terms of the classical diffusion equation. This serves as a prelude to a discussion on fractional diffusion as presented in Section 8, which provides a solution to the problem when multiple scattering effects are present but, as random walk events, conform to a Lévy distribution rather than a normal distribution. The results are presented within the context of the evolution equation for the density field—the density of a canonical ensemble of particles (photons or electrons, for example) undergoing random walk processes.

Having introduced the fractional diffusion equation and the associated solution methods, Section 9 revisits the quantum shutter problem for the classical Schrödinger equation and the extension of the problem to include the space-fractional and then the time-fractional Schrödinger equation. In Section 10, we consider the relativistic case and study the quantum shutter problem for a fractional quantum field described by the fractional Klein–Gordon equation. Finally, Section 11 provides a summary of the material presented and some directions for future research.

1.3. Original Contributions

Judging from the open literature, and, to the best of the authors' knowledge, the approach taken in this paper is original in terms of both the type and style of the review material that is presented in the earlier part of the paper. Moreover, the models and solutions considered in the latter part of the paper, where the focus is on the solution to

fractional differential equations in relation to the quantum shutter problem, appear not to have been considered in previous works. This is undertaken from a theoretical point of view alone and includes an approximative approach to computing the Green's functions for the fractional differential equations considered coupled with the application of a memory function for defining time-fractional derivatives. In this respect, and, in a broader perspective, the study provided belongs to the field of analytical and numerical solutions to fractional differential equations [20].

In addition to the principal theme of the work, an exact solution to the Schrödinger scattering problem is proposed for investigating multiple scattering problems. This complements the use of the random walk models that are considered to address classical and fractional diffusion processes. Finally, a 'fractional Klein–Gordon equation' is proposed to investigate the shutter problem for a 'semi-relativistic' field.

The overall aim of the paper has been to consider a range of physical effects associated with the interaction of a QM field with a shutter in such a way that a unified theme is evolved in regard to studying the dynamics of standard and non-standard quantum fields. The advantages of the approach considered relate to the use of the Green's functions for solving the fractional partial differential equations considered. These Green functions are based on the application of conditions for studying a field close to the shutter over short time periods. The Green's functions constructed in this case are shown to be compatible with those for the conventional equations when the fractional differential reduces to the integer differential. The disadvantage of this approach is that the solutions are constrained by the approximations and conditions that are applied. However, the approach considered provides Green's function solutions that can relatively easily be investigated numerically (examples of which are presented in the paper) that transcend a numerical evaluation of the Mittag–Leffler function, for example.

2. Mathematical Preliminaries

For the purpose of completeness and internal referencing, the mathematical preliminaries associated with the material are provided. Some of the results are standard, while others are non-standard; in either case, some selected references are given as to where the results are provided.

2.1. The Fourier Transform

For a square integrable function $f(\mathbf{r}) \in L^2(\mathbb{R}^n) : \mathbb{C} \rightarrow \mathbb{C}$, and, taken over a Schwartz tempered distributional space, we define the Fourier and inverse Fourier transforms in the 'non-unitary form' as

$$F(\mathbf{k}) = \mathcal{F}_n[f(\mathbf{r})] \equiv \int_{-\infty}^{\infty} f(\mathbf{r}) \exp(-i\mathbf{k} \cdot \mathbf{r}) d^n \mathbf{r}$$

and

$$f(\mathbf{r}) = \mathcal{F}_n^{-1}[F(\mathbf{k})] \equiv \frac{1}{(2\pi)^n} \int_{-\infty}^{\infty} F(\mathbf{k}) \exp(i\mathbf{k} \cdot \mathbf{r}) d^n \mathbf{k},$$

respectively, where $r \equiv |\mathbf{r}|$ and $k \equiv |\mathbf{k}| = 2\pi/\lambda$ is the spatial frequency for wavelength λ . These integral transforms define a Fourier transform pair, which, in this paper, is written using the notation

$$F(\mathbf{k}) \xleftrightarrow{\mathcal{F}_n} f(\mathbf{r})$$

For a function of time t denoted by $f(t)$, the notation becomes

$$F(\omega) \xleftrightarrow{\mathcal{F}} f(t)$$

where

$$F(\omega) = \mathcal{F}[f(t)] \equiv \int_{-\infty}^{\infty} f(t) \exp(-i\omega t) dt$$

$$f(t) = \mathcal{F}^{-1}[F(\omega)] \equiv \frac{1}{2\pi} \int_{-\infty}^{\infty} F(\omega) \exp(i\omega t) d\omega$$

and ω is the temporal (angular) frequency, which is related to a wave speed c_0 and the spatial frequency k by

$$k = \frac{\omega}{c_0}.$$

In this work c_0 is taken to be the speed of light.

2.1.1. The Convolution Integral

For $\mathbf{r} \in \mathbb{R}^n$, the convolution of two functions $f(\mathbf{r})$ and $g(\mathbf{r})$ is defined as

$$s(\mathbf{r}) = g(\mathbf{r}) \otimes_{\mathbf{r}} f(\mathbf{r}) \equiv \int_{-\infty}^{\infty} g(\mathbf{r} - \mathbf{s}) f(\mathbf{s}) d^n \mathbf{s}$$

where $[s(\mathbf{r}), g(\mathbf{r}), f(\mathbf{r})] \in L^2(\mathbb{R}^n) : \mathbb{C} \rightarrow \mathbb{C}$. The dimension associated with this integral operator is taken to be inferred from the dimension of the functions to which the convolution operator is applied. In any dimension, the Convolution Theorem is taken to be applicable, i.e.,

$$g(\mathbf{r}) \otimes_{\mathbf{r}} f(\mathbf{r}) \leftrightarrow G(\mathbf{k}) F(\mathbf{k})$$

where

$$G(\mathbf{k}) \xleftrightarrow{\mathcal{F}_n} g(\mathbf{r}) \text{ and } F(\mathbf{k}) \xleftrightarrow{\mathcal{F}_n} f(\mathbf{r})$$

For a function of time, the following notation is used

$$s(t) = g(t) \otimes_t f(t) = \int_{-\infty}^{\infty} g(t - \tau) f(\tau) d\tau$$

where \otimes_t denotes the (non-causal) convolution integral in time.

2.1.2. The Dirac Delta Function

For $\mathbf{r} \in \mathbb{R}^n$, we define the (n -dimensional) Dirac delta function as

$$\delta^n(\mathbf{r}) = \mathcal{F}_n^{-1}[1] \equiv \frac{1}{(2\pi)^n} \int_{-\infty}^{\infty} \exp(i\mathbf{k} \cdot \mathbf{r}) d^n \mathbf{k} \quad (1)$$

where

$$f(\mathbf{r}) = \delta^n(\mathbf{r}) \otimes_{\mathbf{r}} f(\mathbf{r})$$

2.1.3. Specific Fourier Transform Pairs

The following standard Fourier transforms are used in this paper and are available in standard Fourier transform tables and/or at [21]:

$$\text{sgn}(x) \xleftrightarrow{\mathcal{F}_1} \frac{2}{ik}; \quad \text{sgn}(x) = \begin{cases} 1, & x > 0; \\ -1, & x < 0; \\ 0, & x = 0. \end{cases} \quad (2)$$

$$H(x) \xleftrightarrow{\mathcal{F}_1} 2\pi\delta(k) + \frac{1}{ik}; \quad H(x) = \frac{1}{2}[1 + \operatorname{sgn}(x)] = \begin{cases} 1, & x > 0; \\ 0, & x < 0; \end{cases} \quad \frac{d}{dx}H(x) = \delta(x) \quad (3)$$

$$f^{(n)}(x) \equiv \frac{d^n}{dx^n}f(x) = \delta^{(n)} \otimes_x f(x) \xleftrightarrow{\mathcal{F}_1} (ik)^n F(k), \quad n = 0, 1, 2, 3, \dots \quad (4)$$

$$f^{(\alpha)}(x) \equiv \frac{d^\alpha}{d|x|^\alpha}f(x) \xleftrightarrow{\mathcal{F}_1} |k|^\alpha F(k), \quad 0 < \alpha < 1, \quad x \in (-\infty, \infty) \quad (5)$$

$$f^{(\gamma)}(x) \equiv \frac{d^\gamma}{d|x|^\gamma}f(x) \xleftrightarrow{\mathcal{F}_1} -|k|^\gamma F(k), \quad 1 < \gamma < 2, \quad x \in (-\infty, \infty) \quad (6)$$

$$\exp(-\alpha x^2) \xleftrightarrow{\mathcal{F}_1} \sqrt{\frac{\pi}{\alpha}} \exp\left(-\frac{x^2}{4\alpha}\right) \quad (7)$$

2.2. The Laplace Transformation

The Laplace and inverse Laplace transforms are defined as [22]

$$F(s) = \mathcal{L}[f(t)] \equiv \int_0^\infty f(t) \exp(-st) dt$$

and

$$f(t) = \mathcal{L}^{-1}[F(s)] \equiv \frac{1}{2\pi i} \int_{0^+ - i\infty}^{0^+ + i\infty} F(s) \exp(st) ds,$$

respectively. The Laplace transform of function $f(t)$ exists only if

$$\int_{-\infty}^\infty |f(t) \exp(-st)| dt < \infty$$

or only if

$$\lim_{t \rightarrow \infty} [f(t) \exp(-st)] = 0$$

Thus, the necessary and sufficient conditions for the existence of the Laplace transform are, respectively, that (i) the function $f(t)$ should be piece-wise continuous in the given closed interval and must be of an exponential order; and (ii) the function $f(t) \exp(-st)$ should be absolutely integrable.

The Laplace transform pair is implied using the notation

$$F(s) \xleftrightarrow{\mathcal{L}} f(t)$$

for which the following fundamental results are applicable:

$$f(t) \otimes_t g(t) \xleftrightarrow{\mathcal{L}} F(s)G(s)$$

and

$$\delta(t) \xleftrightarrow{\mathcal{L}} 1$$

where \otimes_t denotes the causal convolution integral (in association with the Laplace transform alone and not the Fourier transform)

$$g(t) \otimes_t f(t) \equiv \int_0^t g(t-\tau)f(\tau)d\tau$$

The following specific Laplace transforms pairs are used in this paper and are available in standard Laplace transform tables and/or at [23]:

$$\frac{1}{s^\alpha} \xleftrightarrow{\mathcal{L}} \frac{1}{\Gamma(\alpha)} \frac{1}{t^{1-\alpha}}, \operatorname{Re}[\alpha] < 1; \quad \Gamma(\alpha) = \int_0^\infty x^{\alpha-1} \exp(-x) dx, \quad \Gamma(1+\alpha) = \alpha\Gamma(\alpha) \quad (8)$$

$$s^\alpha \xleftrightarrow{\mathcal{L}} \frac{1}{\Gamma(-\alpha)} \frac{1}{t^{1+\alpha}}, \operatorname{Re}[\alpha] > -1 \quad (9)$$

$$\frac{1}{\sqrt{s}} \exp(-x\sqrt{s}) \xleftrightarrow{\mathcal{L}} \frac{1}{\sqrt{\pi t}} \exp\left(-\frac{x^2}{4t}\right) \quad (10)$$

$$f^{(n)}(t) \equiv \frac{d^n}{dt^n} f(t) \xleftrightarrow{\mathcal{L}} s^n F(s) - \sum_{m=1}^n s^{n-m} f^{(m-1)}(0) \quad (11)$$

$$f^{(\alpha)}(t) \equiv \frac{d^\alpha}{dt^\alpha} f(t) \xleftrightarrow{\mathcal{L}} s^\alpha F(s) - \sum_{m=0}^{n-1} s^{\alpha-m-1} f^{(m)}(0) \quad (12)$$

$$\exp(-\alpha t) H(t) \xleftrightarrow{\mathcal{L}} \frac{1}{s + \alpha} \quad (13)$$

A proof of the non-standard Relationship (12) is given in [24], for example.

2.3. Green's Function

For the classical diffusion operator $D\nabla^2 - \partial_t$, where ∇^2 is the Laplacian differential operator and D is the diffusivity, the Green's functions are given by [2]

$$G(\mathbf{r}, t) = H(t) \left(\frac{1}{4\pi Dt} \right)^{\frac{n}{2}} \exp\left(-\frac{r^2}{4Dt}\right), \quad \mathbf{r} \in \mathbb{R}^n \quad (14)$$

For the homogeneous Helmholtz operator $\nabla^2 + k^2$, the time-independent and outgoing Green's functions, for $\mathbf{r} \in \mathbb{R}^n$, are given by (functions of $r \equiv |\mathbf{r}|$) [2]

$$g(r, k) = \begin{cases} \frac{i}{2k} \exp(ikr), & n = 1; \\ \frac{i}{4} H_0^{(1)}(kr), & n = 2; \\ \frac{1}{4\pi r} \exp(ikr), & n = 3. \end{cases} \quad (15)$$

2.4. p - and Uniform-Norms

We define the p -norm as

$$\|f(\mathbf{r})\|_p \equiv \left(\int_{\mathbf{r} \in \mathbb{R}^n} |f(\mathbf{r})|^p d^n \mathbf{r} \right)^{\frac{1}{p}}, \quad 1 \leq p \leq \infty$$

with the uniform norm being defined as

$$\|f(\mathbf{r})\|_\infty = \sup\{|f(\mathbf{r})|, \mathbf{r} \in \mathbb{R}^n\}$$

and standard properties:

$$\|f(\mathbf{r}) + g(\mathbf{r})\|_p \leq \|f(\mathbf{r})\|_p + \|g(\mathbf{r})\|_p \quad (16)$$

$$\|f(\mathbf{r})g(\mathbf{r})\|_p \leq \|f(\mathbf{r})\|_p \|g(\mathbf{r})\|_p \quad (17)$$

and

$$\|f(\mathbf{r}) \otimes_{\mathbf{r}} g(\mathbf{r})\|_p \leq \|f(\mathbf{r})\|_p \|g(\mathbf{r})\|_p \quad (18)$$

2.5. Field Notation

Throughout this work, the field, whose solution is sought, is denoted by $u(\mathbf{r}, t)$. This function may be the wave-field for a scalar electromagnetic field or a quantum field describing a photon or an electron, respectively, for example. In this case, the measurable quantity is taken to be given by $|u(\mathbf{r}, t)|^2$ (the probability density). However, $u(\mathbf{r}, t)$ is also used to represent the density field which is the number of particles (photons or electrons, for example) per unit dimension. The difference in the physical meaning of $u(\mathbf{r}, t)$ is inferred through the context in which the physical models are considered, and the governing equations and the solutions thereof that are addressed.

2.6. Units

Some of the analysis provided in the latter part of this work involves the development of solutions to equations for which ‘Natural units’ (for particle and atomic physics) are applied. In this case, the speed of light c_0 , the Dirac constant \hbar , and the electron mass m are all taken to be equal to 1, i.e.,

$$c_0 = \hbar = m = 1$$

In the construction of a fractional derivative, a scaling parameter is required to maintain the dimensionality of the equation which can then be set to 1. Thus, for example, consider the first order spatial derivative $df(x)/dx$ of a dimensionless function $f(x)$. The dimensions of this derivative are $1/L$ (the reciprocal of length L), but the fractional derivative $d^\alpha f(x)/dx^\alpha$, $0 < \alpha < 1$, say, has dimensions of $1/L^\alpha$. In order to maintain the dimensionless nature of the function $f(x)$ that is being fractionally differentiated, it is necessary to introduce an appropriate scaling factor η (a real constant with the dimensions of L) raised to an appropriate fractional power. Thus, in this particular example, the fractional derivative is written as $\eta^{\alpha-1} d^\alpha f(x)/dx^\alpha$. However, for $\eta = 1$, the introduction of this notation is null and void and can be merely inferred in relation to preserving the dimensionality of the original (non-fractional) differential.

3. Fractional Partial Differential Equations and the Mittag–Leffler Function

Fractional partial differential equations and their solutions critically depend on the definition(s) that are applied for a fractional differential, and, more specifically, a fractional differo-integral operator. There are a wide range of conventional definitions for such operators, such as the Riemann–Liouville fractional integral and the Caputo fractional derivative [25]. Moreover, there are a broad range of generalised definitions, leading to the issue as to how many fractional derivative there are [26], and, whether there is an upper bound to the number of definition that can, in principle, be constructed, as discussed in [25]. Such definitions often depend upon whether they should incur a boundary and/or initial condition that is consistent with the physical model that is being considered. This is of particular importance in regard to time-fractional differential equations involving a fundamental solution using the Green’s function through the application of a Fourier transform of a function over space and a Laplace transformation over time. In regard to the latter case, the Mittag–Leffler function [19] is often used to study the effect of initial conditions in regard to time-fractional control problems. The following sections provide an example of this in regard to solving the fractional diffusion equation.

3.1. Fourier–Laplace Transform Solution to the Diffusion Equation

Consider the one-dimensional classical diffusion equation (for unit Diffusivity)

$$\left(\frac{\partial^2}{\partial x^2} - \frac{\partial}{\partial t} \right) u(x, t) = 0, \quad u(x, t = 0) = u_0(x)$$

where we require a Green's function solution for $u(x, t)$, $x \in (-\infty, \infty)$, $t > 0$, subject to the condition that $u(x, t) \rightarrow 0$ as $|x| \rightarrow \infty$.

The standard approach to solving this problem is to apply the Fourier and Laplace transforms. Defining the transformed function as

$$\bar{U}(k, s) = \int_{-\infty}^{\infty} dx \exp(-ikx) \int_0^{\infty} dt \exp(-st) u(x, t)$$

and using Relationships (4) and (11), the diffusion equation becomes (in Fourier–Laplace space)

$$-k^2 \bar{U}(k, s) - [s \bar{U}(k, s) - U_0(k)] = 0$$

so that we can write

$$\bar{U}(k, s) = \frac{U_0(k)}{k^2 + s}$$

The solution is then given by computing the inverse Fourier and inverse Laplace transforms to this equation, which, in principle, can be done in any order. Taking the inverse Laplace transform first and using Relationship (13),

$$U(k, t) = U_0(k) \exp(-k^2 t), \quad t > 0$$

and using Relationship (7) together with the convolution theorem, we obtain [2]

$$u(x, t) = u_0(x) \otimes_x \frac{1}{\sqrt{4\pi t}} \exp\left(-\frac{x^2}{4t}\right)$$

This result is a convolution in space with the Green's function, i.e.,

$$u(x, t) = u_0(x) \otimes_x G(x, t)$$

where $G(x, t)$ is given by Equation (14) for $n = 1$.

3.2. Fourier–Laplace Transform Solution to the Time-Fractional Diffusion Equation

Let us now repeat this analysis given in the previous section for the time-fractional diffusion equation

$$\left(\frac{\partial^2}{\partial x^2} - \frac{\partial^\alpha}{\partial t^\alpha} \right) u(x, t), \quad u(x, t = 0) = u_0(x), \quad 0 < \alpha < 1$$

subject to the same asymptotic conditions. In this case, following the same transformations, and using Relationship (12), we obtain

$$\bar{U}(k, s) = \frac{U_0(k) s^{\alpha-1}}{k^2 + s^\alpha} \quad (19)$$

To obtain an expression for $U(k, t)$, the inverse Laplace transform of the function $s^{\alpha-1}/(s^\alpha + k^2)$ is now required; this is where the Mittag–Leffler plays an essential role.

3.3. The Mittag–Leffler and Wright Functions

The Mittag–Leffler function is defined as [19]

$$E_{\alpha, \beta}(z) = \sum_{n=0}^{\infty} \frac{z^n}{\Gamma(\alpha n + \beta)}, \quad \alpha > 0, \quad \beta > 0$$

and, importantly, has the Laplace transform relationship [24]

$$E_{\alpha,\beta}(z) \xleftrightarrow{\mathcal{L}} \frac{s^{\alpha-\beta}}{s^\alpha - z}.$$

This result immediately allows the inverse Laplace transform of $\bar{U}(k, s)$, as given by Equation (19), to be written as

$$U(k, t) = U_0(k) E_{\alpha,1}(-k^2 t^\alpha)$$

so that the solution required becomes

$$u(x, t) = u_0(x) \otimes_x G_\alpha(x, t) \quad (20)$$

where

$$G_\alpha(x, t) = \frac{1}{2\pi} \int_{-\infty}^{\infty} E_{\alpha,1}(-k^2 t^\alpha) \exp(ikx) dk = \frac{1}{2t^{\alpha/2}} M_\alpha\left(\frac{|x|}{t^{\alpha/2}}\right) \quad (21)$$

and $M_\alpha(z)$ is the Wright function [27],

$$M_\alpha(z) = \sum_{n=0}^{\infty} \frac{(-z)^n}{n! \Gamma(-\alpha n + 1 - \alpha)}.$$

The geometry of convergence in regard to the Mittag-Leffler function is studied in [28].

3.4. Discussion

The Mittag-Leffler and Wright functions used to develop the Green's function solution to the time-fractional diffusion equation can be applied to solve other partial differential equations including the time-fractional Schrödinger equation [29]. Both these functions are non-standard or 'special functions' which involve definitions based on infinite series. Nevertheless, the numerical evaluation of such functions is available from different sources, e.g., [30,31]. This provides the facility for investigating Equation (20) numerically, based on the application of a discrete convolution operation. On the other hand, it is arguable that the inverse Fourier and Laplace transforms are applied numerically to compute $u(x, t)$ from Equation (19) directly, thereby by-passing the need to introduce such non-standard functions and their numerical evaluation. In this context, the approach taken in this paper follows an evaluation of the Green's functions based on various asymptotic's that are specifically designed to obtain Green's function of the type given by Equation (14). This is coupled with a definition of a fractional time derivative that is based on introducing an appropriate memory function $m(t)$, where (for a causal convolution operator \otimes_t)

$$\frac{\partial^\alpha}{\partial t^\alpha} u(x, t) = m(t) \otimes_t \frac{\partial}{\partial t} u(x, t)$$

4. Review of Diffraction in Space for an Open Shutter—Diffraction by an Aperture

The purpose of this section is to provide the context to the 'Diffraction in Time' phenomenon. This is done by first re-visiting the basic mathematical foundations of diffraction theory, which provides a connectivity between diffraction in space and diffraction in time—essentially, time-independent and time-dependent diffraction, respectively. In this sense, the term 'Diffraction' can refer to a light beam or an electron beam or any other elementary 'particle' beam, at least in the context of the non-relativistic and spin-less case, when particles propagate at a speed much less than light speed. Although the models for diffraction in space are well known, it is revisited in this section so that the reader is made aware of both the differences and basic similarities between the spatial diffraction of an electromagnetic wave and a (non-relativistic) electron wave 'oscillating' at a fixed frequency.

With reference to Figure 1, let us consider the case when the shutter is permanently open, thereby producing an aperture. If the width of the incident wave-field in the negative half space is less than the width of the aperture, then one would expect the beam to travel through the aperture and continue propagating (from left to right) into the positive half space $x \in [0, \infty)$. In this context, if the shutter remains closed, then the positive half space will remain free of any wave-field. However, if the beam width is larger than, or at least equal to, the width of the aperture, then part of the wave-field will interact with the edges of the aperture. It is this interaction that produces a diffraction pattern in the positive half-space. The characteristics of this pattern (measured over the coordinate y , say) will depend on the distance in x away from the aperture at $x = 0$, over which the wave-field is detected (as a function of y). In this case, (x, y) defines the coordinates in the positive (and negative) half-space. It is this issue that is now considered in terms of the basic mathematical formulation of the diffraction patterns that occur in the ‘far-field’ (the ‘Fourier plane’) and the ‘intermediate-field’ (the ‘Fresnel zone’), which is undertaken for the two-dimensional case when $\mathbf{r} \in \mathbb{R}^2$.

4.1. Electromagnetic Wave Equation

A light wave (or any other electromagnetic wave, representing a stream of photons) propagating in a free space at the speed of light c_0 , is governed by the homogeneous wave equation

$$\left(\nabla^2 - \frac{1}{c_0^2} \frac{\partial^2}{\partial t^2} \right) u(\mathbf{r}, t) = 0 \quad (22)$$

This is a scalar model for the electric or magnetic field represented by the wave-field $u(\mathbf{r}, t)$. For $\mathbf{r} \in \mathbb{R}^2$, and, for unit vectors $\hat{\mathbf{x}}$ and $\hat{\mathbf{y}}$,

$$\mathbf{r} = \hat{\mathbf{x}}x + \hat{\mathbf{y}}y, \quad \nabla^2 \equiv \frac{\partial^2}{\partial x^2} + \frac{\partial^2}{\partial y^2}$$

and $u(\mathbf{r}, t)$ is the Electric or Magnetic field in a two-dimensional space. This model is restrictive, as polarisation effects, due to the fact that electric and magnetic fields are vector fields, are not incorporated. Moreover, the model is two-dimensional. However, the purpose of this section is to contextualise the phenomenon of (spatial) diffraction in terms of the model illustrated in Figure 1. It is for this reason that a two-dimensional scalar wave-field model for diffraction is considered.

4.1.1. Time Harmonic Equation

If we consider the wave-field to be harmonic in time when we can write $u(\mathbf{r}, t) = U(\mathbf{r}, \omega) \exp(i\omega t)$ where ω is a constant (angular) frequency, then we can consider the time-independent (homogenous Helmholtz) equation

$$\left(\nabla^2 + k^2 \right) U(\mathbf{r}, \omega) = 0, \quad k = \frac{\omega}{c_0} = \frac{2\pi}{\lambda} \quad (23)$$

where λ is the wavelength. Note that this equation applies equally well for the case when there is a frequency spectrum, given that, in this case,

$$u(\mathbf{r}, t) \xleftrightarrow{\mathcal{F}} U(\mathbf{r}, \omega)$$

where $u(\mathbf{r}, t)$ and $U(\mathbf{r}, \omega)$ are Fourier transform pairs, i.e.,

$$u(\mathbf{r}, t) = \frac{1}{2\pi} \int_{-\infty}^{\infty} U(\mathbf{r}, \omega) \exp(i\omega t) d\omega \quad \text{and} \quad U(\mathbf{r}, \omega) = \int_{-\infty}^{\infty} u(\mathbf{r}, t) \exp(-i\omega t) dt$$

For a wave-field $U(\mathbf{r}, \omega)$ with a characteristic spectrum $P(\omega)$ say, and using the convolution theorem,

$$u(\mathbf{r}, t) = \frac{1}{2\pi} \int_{-\infty}^{\infty} U(\mathbf{r}, \omega) P(\omega) \exp(i\omega t) d\omega = u(\mathbf{r}, t) \otimes_t p(t) \equiv \int_{-\infty}^{\infty} u(\mathbf{r}, t - \tau) p(\tau) d\tau$$

where \otimes_t denotes the (non-causal) convolution integral in time. Thus, for a spectrum consisting of a single frequency ω_0 , if we let $P(\omega) = 2\pi\delta(\omega - \omega_0)$, then

$$u(\mathbf{r}, t) = \int_{-\infty}^{\infty} U(\mathbf{r}, \omega) \delta(\omega - \omega_0) \exp(i\omega t) d\omega = U(\mathbf{r}, \omega_0) \exp(i\omega_0 t)$$

thereby recovering the time harmonic case for constant frequency ω_0 . In this case, the wave-field is taken to oscillate at the same frequency for all time and only the spatial characteristics of the wave-field $U(\mathbf{r}, \omega)$ are considered (for constant ω). No initial conditions for the field $u(\mathbf{r}, t)$ and/or its gradient, when we need to specify the values of $u(\mathbf{r}, t)$ and/or $\partial u(\mathbf{r}, t)/\partial t$ at $t = 0$, respectively, are relevant. The model therefore relates to a non-causal system and there are no initial conditions in time that control any time evolution of the ‘system’.

4.1.2. Inhomogeneous Helmholtz Equation

With reference to Figure 1, we consider the case when the incident beam interacts with the edges of the aperture. While the frequency is constant, in regard to Equation (23), this interaction can be taken to slightly reduces the propagation speed, which is strictly less than light speed. Thus, in a general context, the light speed is inhomogeneous in space over the region of the aperture. We can model this inhomogeneity by replacing $1/c_0^2$ in Equation (22) with

$$\frac{1}{c^2(\mathbf{r})} = \frac{1}{c_0^2} [1 + V(\mathbf{r})]$$

so that, if $V(\mathbf{r}) = 0$, $\forall \mathbf{r}$, then the space is homogenous. In this case, Equation (23) becomes (the inhomogeneous Helmholtz equation)

$$(\nabla^2 + k^2)U(\mathbf{r}, k) = -k^2 V(\mathbf{r})U(\mathbf{r}, k) \quad (24)$$

and it is this equation that we now need to solve for $U(\mathbf{r}, k)$ given $V(\mathbf{r})$, which is taken to be of compact support.

This result is of course based on considering the conversion of a constant wave-speed to a variable wave-speed and has been achieved in a phenomenological context. However, by decoupling the macroscopic Maxwell’s equation it can be shown that, if the aperture is a non-conductive dielectric, then $V(\mathbf{r}) = \epsilon_r(\mathbf{r}) - 1$, where $\epsilon_r \geq 1$ is the relative permittivity (ignoring polarisation effects) [3]. Similarly, if the aperture is a conductive dielectric, then $V(\mathbf{r}) = \epsilon_r - 1 - iz_0\sigma(\mathbf{r})/k$ where σ is the conductivity and z_0 is impedance of free space [3]. In either case, the relative permeability is taken to be that of free space and $U(\mathbf{r}, k)$ is taken to be the electric field.

4.2. Non-Relativistic Quantum Wave Equation

For the non-relativistic case, an electron wave $u(\mathbf{r}, t)$, say, propagating in an n -dimensional free space, is described by the Schrödinger equation

$$\left(\frac{\hbar^2}{2m} \nabla^2 + i\hbar \frac{\partial}{\partial t} \right) u(\mathbf{r}, t) = 0 \quad (25)$$

where \hbar is the Dirac constant and m is the electron mass. Here, the operator $i\hbar\partial_t$ is associated with the energy $E = \hbar\omega$ of the electron wave-field $u(\mathbf{r}, t)$.

If an electron beam is incident upon an open aperture, the edges of the aperture represent a potential energy $V(\mathbf{r})$ of space \mathbf{r} , and, given that the total energy is given by $E - V$, then from Equation (25), we obtain the inhomogeneous equation

$$\left(\frac{\hbar^2}{2m} \nabla^2 + i\hbar \frac{\partial}{\partial t} \right) u(\mathbf{r}, t) = V(\mathbf{r})u(\mathbf{r}, t)$$

Thus, for harmonic time variations in the wave-field $u(\mathbf{r}, t)$ at a frequency ω , we can again consider the case where $u(\mathbf{r}, t) = U(\mathbf{r}, \omega) \exp(-i\omega t)$ giving (the time-independent inhomogeneous Schrödinger equation)

$$(\nabla^2 + k^2)U(\mathbf{r}, k) = V(\mathbf{r})U(\mathbf{r}, k) \quad (26)$$

where $k^2 = 2mE/\hbar^2$ and $V(\mathbf{r}) := 2mV(\mathbf{r})/\hbar^2$.

Comparing Equation (24) with Equation (26), the basic differences lie in the definitions of k and $V(\mathbf{r})$ and whether or not $-k^2$ is a coefficient of $V(\mathbf{r})$, respectively. Thus, for constant k , any solution acquired for $U(\mathbf{r}, k)$ is the same in either case. In both cases, the time-independent equation describes a non-causal system with no time controlling properties and associated initial conditions. The fundamental solutions to these equations are now considered.

5. Fundamental Solution: The Green's Function Solution

Since, for constant k , Equations (24) and (26) are effectively the same, we consider the Green's function solution to Equation (26). This is given by the Lippmann-Schwinger equation [2]

$$U(\mathbf{r}, k) = U_i(\mathbf{r}, k) + U_s(\mathbf{r}, k) \quad (27)$$

where $U_s(\mathbf{r}, k)$ is the field scattered by the 'scattering function' $V(\mathbf{r})$ given by

$$U_s(\mathbf{r}, k) = g(r, k) \otimes_{\mathbf{r}} V(\mathbf{r})U(\mathbf{r}, k) \equiv \int_{-\infty}^{\infty} g(|\mathbf{r} - \mathbf{s}|, k) V(\mathbf{s}) U(\mathbf{s}, k) d^2\mathbf{s} \quad (28)$$

and $\otimes_{\mathbf{r}}$ denotes the two-dimensional convolution integral for $\mathbf{r} \in \mathbb{R}^2$.

The function $g(r, k)$ (where $r = |\mathbf{r}|$) is the two-dimensional 'outgoing' free space Green's function, which is the solution to

$$(\nabla^2 + k^2)g(r, k) = \delta^2(\mathbf{r})$$

for two-dimensional Dirac delta function $\delta^2(\mathbf{r})$. The 'incident wave-field' $U_i(\mathbf{r}, k)$ is taken to be the solution to the homogeneous Helmholtz equation

$$(\nabla^2 + k^2)U_i(\mathbf{r}, k) = 0 \quad (29)$$

Equation (27) is a fundamental solution to Equation (26) since

$$\begin{aligned} \nabla^2 U(\mathbf{r}, k) &= \nabla^2 U_i(\mathbf{r}, k) + \nabla^2 [g(r, k) \otimes_{\mathbf{r}} V(\mathbf{r})U(\mathbf{r}, k)] \\ &= \nabla^2 U_i(\mathbf{r}, k) + \nabla^2 g(r, k) \otimes_{\mathbf{r}} V(\mathbf{r})U(\mathbf{r}, k) \\ &= \nabla^2 U_i(\mathbf{r}, k) + [\delta^2(r) - k^2 g(r, k)] \otimes_{\mathbf{r}} V(\mathbf{r})U(\mathbf{r}, k) \\ &= \nabla^2 U_i(\mathbf{r}, k) + V(\mathbf{r})U(\mathbf{r}, k) - k^2 [U(\mathbf{r}, k) - U_i(\mathbf{r}, k)] \\ &= -k^2 U(\mathbf{r}, k) + V(\mathbf{r})U(\mathbf{r}, k) \end{aligned} \quad (30)$$

given that

$$\delta^2(r) \otimes_{\mathbf{r}} V(\mathbf{r})U(\mathbf{r}, k) = V(\mathbf{r})U(\mathbf{r}, k)$$

For $\mathbf{r} \in \mathbb{R}^2$, the Green's function is given by [2]

$$g(r, k) = \frac{i}{4\pi} \int_0^\pi \exp(ikr \cos \theta) d\theta = \frac{i}{4} H_0^{(1)}(kr)$$

where $H_0^{(1)}$ is the Hankel function of the first kind and of order zero given by

$$H_0^{(1)}(kr) = \frac{1}{\pi} \int_0^\pi \exp(ikr \cos \theta) d\theta \sim \sqrt{\frac{2}{\pi}} \exp(-i\pi/4) \frac{\exp(ikr)}{\sqrt{kr}} \quad (31)$$

Thus, the asymptotic form for the two-dimensional Green's function is

$$g(r, k) = \frac{\exp(i\pi/4)}{\sqrt{8\pi}} \frac{\exp(ikr)}{\sqrt{kr}} \quad (32)$$

Application of this conditional form is valid when $kr \gg 1$ so that the wavelength of the wave-field is small compared to the distance between the point source of the field $\delta^2(r)$ and the position r at which the field is observed.

5.1. Solutions under the Born Approximation

Equation (27) is an integral equation of Fredholm type and has a range of solution method for evaluating $U(\mathbf{r}, k)$. The simplest and most common (approximate) solution to this equation is obtained by applying what is commonly referred to as the Born approximation [2]. This is where it is assumed that the convolution integral can be approximated by $g(r, k) \otimes_{\mathbf{r}} V(\mathbf{r}) U_i(\mathbf{r}, k)$. Application of this approximation requires that (for some norm denoted by $\|\bullet\|$)

$$\frac{\|U_s(\mathbf{r}, k)\|}{\|U_i(\mathbf{r}, k)\|} \ll 1 \quad (33)$$

where the Born scattered field is given by

$$U_s(\mathbf{r}, k) = g(r, k) \otimes_{\mathbf{r}} V(\mathbf{r}) U_i(\mathbf{r}, k) \quad (34)$$

The Born scattering condition given above implies that the scattering is a 'weak effect', i.e., the scattered field is a small perturbation of the incident field. In physical terms, this means that there are no multiple scattering effects taken to be present. Thus, the Born scattered field is a model for single scattering events alone. A quantification of this condition will be considered later.

Multiple scattering events can be taken into account through iteration of Equation (27) (the first iteration being the Born scattered field), which requires that the series converges [2]. This is a formal solution to the scattering problem, a problem that has been studied over many years. In this context, Appendix A provides a complementary solution to Equation (27) for $\mathbf{r} \in \mathbb{R}^n$, coupled with a short study on the type of functions to which $V(\mathbf{r})$ must conform, for the solution(s) to be valid.

Given that $U_i(\mathbf{r}, k) = \exp(i\mathbf{k} \cdot \mathbf{r})$ is a solution to Equation (29), the Born scattered field can be written as (for $\mathbf{r} \in \mathbb{R}^2$)

$$U_s(\mathbf{r}, k) = \frac{\exp(i\pi/4)}{\sqrt{8\pi}} \frac{\exp(ikr)}{\sqrt{kr}} \otimes_{\mathbf{r}} V(\mathbf{r}) \exp(i\mathbf{k}\hat{\mathbf{m}} \cdot \mathbf{r}), \text{ where } \hat{\mathbf{m}} = \frac{\mathbf{k}}{k}, k = |\mathbf{k}|$$

It is assumed that the incident field $U_i(\mathbf{r}, k)$ is a unit plane wave, but the solution to Equation (29) applies to any plane wave with arbitrary amplitude, an amplitude that may also be a function of k .

The evaluation of the scattered field $U_s(\mathbf{r}, k)$ now depends on an analysis of the function $\exp(ikr)/\sqrt{r}$ as a kernel of the convolution integral, i.e., Equation (28). This analysis is based on noting that (where $s = |\mathbf{s}|$)

$$|\mathbf{r} - \mathbf{s}| = \sqrt{(\mathbf{r} - \mathbf{s}) \cdot (\mathbf{r} - \mathbf{s})} = (r^2 + s^2 - 2\mathbf{r} \cdot \mathbf{s})^{\frac{1}{2}} = r \left(1 - 2\frac{\mathbf{r} \cdot \mathbf{s}}{r^2} + \frac{s^2}{r^2} \right)^{\frac{1}{2}} \\ \sim r \left(1 - \frac{\mathbf{r} \cdot \mathbf{s}}{r^2} + \frac{s^2}{2r^2} + \dots \right)$$

The difference between evaluating the scattered field in the Fourier or Fresnel zones is dependent on the incorporation of just the second or the second and third terms of the binomial series given above, as shall now be demonstrated.

5.1.1. Scattering Amplitude in the Fourier Zone

If we assume that $s/r \ll 1$, then the term $s^2/2r^2$ and higher order terms in the binomial series can be ignored. We can then consider the result

$$\frac{\exp(ik|\mathbf{r} - \mathbf{s}|)}{\sqrt{k|\mathbf{r} - \mathbf{s}|}} = \frac{\exp(ikr)}{\sqrt{kr}} \exp(-ik\hat{\mathbf{n}} \cdot \mathbf{s}), \text{ where } \hat{\mathbf{n}} = \frac{\mathbf{r}}{r}$$

In this case, the scattered field is given by

$$U_s(\mathbf{r}, k) = \frac{\exp(i\pi/4)}{\sqrt{8\pi}} \frac{\exp(ikr)}{\sqrt{kr}} A[k(\hat{\mathbf{n}} - \hat{\mathbf{m}})]$$

where

$$A[k(\hat{\mathbf{n}} - \hat{\mathbf{m}})] = \int_{-\infty}^{\infty} \exp[-ik(\hat{\mathbf{n}} - \hat{\mathbf{m}}) \cdot \mathbf{s}] V(\mathbf{s}) d^2\mathbf{s} \quad (35)$$

is the scattering amplitude. It is immediately clear that the scattering amplitude is, in effect, given by the two-dimensional Fourier transform of $V(\mathbf{r})$.

5.1.2. Scattering Amplitude in the Fresnel Zone

If we assume that the term $r^2/2s^2$ is much less than 1, then only higher order terms after this term can be ignored. In this case, we consider a representation of the complex exponential given by

$$\frac{\exp(ik|\mathbf{r} - \mathbf{s}|)}{\sqrt{k|\mathbf{r} - \mathbf{s}|}} = \frac{\exp(ikr)}{\sqrt{kr}} \exp(-ik\hat{\mathbf{n}} \cdot \mathbf{s}) \exp(iks^2/2r), \quad \frac{r^2}{s^2} \ll 1$$

This result can now be written in the compound form

$$\frac{\exp(ik|\mathbf{r} - \mathbf{s}|)}{\sqrt{k|\mathbf{r} - \mathbf{s}|}} = \frac{\exp(-ikr/2)}{\sqrt{kr}} \exp(ik|\mathbf{r} - \mathbf{s}|^2/2r)$$

given that

$$|\mathbf{r} - \mathbf{s}|^2 = r^2 - 2\mathbf{r} \cdot \mathbf{s} + s^2$$

which allows the scattered field to be written as

$$U_s(\mathbf{r}, k) = \frac{\exp(i\pi/4)}{\sqrt{8\pi}} \frac{\exp(-ikr/2)}{\sqrt{kr}} A(\mathbf{r}, k)$$

where

$$A(\mathbf{r}, k) = \exp(i\alpha|\mathbf{r}|^2) \otimes_{\mathbf{r}} [V(\mathbf{r}) \exp(ik\hat{\mathbf{m}} \cdot \mathbf{r})] \quad (36)$$

and $\alpha = k/2r$ is a constant. Note that the term $k/2r$ is not a variable in the convolution integral but a constant coefficient of the variable $|\mathbf{r} - \mathbf{s}|$.

5.2. Diffraction Patterns

In the context of Figure 1, let us now consider how to construct a model for the diffraction pattern in the Fourier and Fresnel zones.

5.2.1. Diffraction Pattern in the Fourier Zone

The aim is to consider Equation (35) and modify the result in a way that is compatible with the geometry associated with Figure 1, where a one-dimensional screen (upon which the diffraction pattern is taken to be observed as a function of y) is placed a long distance away (in the ‘far-field’) from the aperture so that $x/y \ll 1$. The incident field is taken to be a function of x alone, as it propagates in the x -direction (from left to right, in the negative half-space as illustrated in Figure 1). Thus, given that $\hat{\mathbf{m}} = \hat{\mathbf{x}}$, then $\exp(ik\hat{\mathbf{m}} \cdot \mathbf{r}) = \exp(ikx)$. Furthermore, since we are considering the result in the far-field of the positive (two-dimensional) half-space (x, y) , $x > 0$ then

$$\hat{\mathbf{n}} = \frac{\mathbf{r}}{r} = \frac{\hat{\mathbf{x}}x + \hat{\mathbf{y}}y}{\sqrt{x^2 + y^2}} = \frac{\hat{\mathbf{x}}x + \hat{\mathbf{y}}y}{x\sqrt{1 + \frac{y^2}{x^2}}} \simeq \hat{\mathbf{x}} + \hat{\mathbf{y}}\frac{y}{x}, \quad \frac{y}{x} \ll 1$$

With these results, Equation (35) becomes (using the notation $\mathbf{s} = \hat{\mathbf{x}}s_x + \hat{\mathbf{y}}s_y$, for Cartesian coordinates),

$$\begin{aligned} A(x, y, k) &= \int_{-\infty}^{\infty} \int_{-\infty}^{\infty} V(s_x, s_y) \exp(-iks_x) \exp(-iks_y y/x) \exp(iks_x) ds_x ds_y \\ &= \int_{-\infty}^{\infty} \int_{-\infty}^{\infty} \exp(-iks_y y/x) V(s_x, s_y) ds_x ds_y = \int_{-\infty}^{\infty} \exp(-iks_y y/x) V(s_y) ds_y \end{aligned} \quad (37)$$

where

$$V(s_y) = \int_{-\infty}^{\infty} V(s_x, s_y) ds_x.$$

This result now needs to be further quantified with regard to the function $V(s_x, s_y)$. In terms of an open aperture relating to Figure 1, for a width W and thickness T , we can consider that

$$V(s_x, s_y) = \begin{cases} 1, & |s_x| \leq T; \\ 1, & |s_y| \leq W; \\ 0, & \text{otherwise,} \end{cases}$$

where the aperture is taken to be a unit constant for which values other than 1 may of course be applied. In this context, the ‘otherwise’ condition is simply stating that, apart from the aperture, no radiation can penetrate into the positive half-space as illustrated in Figure 1. Thus, from Equation (37), the scattering amplitude becomes

$$A(K) = T \int_{-W/2}^{W/2} \exp(-iKs_y) ds_y, \quad K = \frac{ky}{x}.$$

It now becomes clear that the diffraction pattern (as a function of y) for a fixed value of x is determined by the one-dimensional Fourier transform of a constant where $s_y \in [-W/2, W/2]$, the measurable intensity pattern being given by $|A(K)|^2$.

There is another approach that can be used to derive what is essentially the same result and involves a model where the aperture is taken to be infinitely thin. However, in order to eliminate the trivial result $A(K) = 0$ if $T = 0$, we resort to the application of a

delta function to model an aperture that is infinitely thin (in a hypothetical context). This is accomplished by considering an expression for $V(s_x, s_y)$ given by

$$V(s_x, s_y) = \delta(s_x)V(s_y)$$

where

$$V(s_y) = \begin{cases} 1, & |s_y| \leq W; \\ 0, & \text{otherwise.} \end{cases}$$

given that (by definition)

$$\int_{-\infty}^{\infty} \delta(s_x) ds_x = 1$$

For this model, the constant T is eliminated, and the scattering amplitude intensity is given by

$$|A(K)|^2 = \left| \int_{-W/2}^{W/2} \exp(-iKs_y) ds_y \right|^2 \quad (38)$$

5.2.2. Diffraction Pattern in the Fresnel Zone

The same basic approach can be used to generate an expression for the diffraction pattern in the Fresnel zone given Equation (36). Specifically, for an infinitely thin aperture and with $\hat{\mathbf{m}} = \hat{\mathbf{x}}$, then, in Cartesian coordinates,

$$\begin{aligned} A(x, y, k) &= \exp(i\alpha x^2) \exp(i\alpha y^2) \otimes_{\mathbf{r}} [\delta(x)V(y) \exp(ikx)] \\ &= \exp(i\alpha x^2) \exp(i\alpha y^2) \otimes_{\mathbf{r}} [\delta(x)V(y) \exp(ikx)] \\ &= \exp(i\alpha x^2) \exp(i\alpha y^2) \otimes_y V(y) \end{aligned}$$

where $\alpha = k/2x$ given that $y/x \ll 1$.

The convolution integral is over y alone and the measurable intensity of the Fresnel diffracted field becomes

$$|A(y)|^2 = \left| \exp(i\alpha y^2) \otimes_y V(y) \right|^2 \quad (39)$$

where

$$V(y) = \begin{cases} 1, & |y| \leq W; \\ 0, & \text{otherwise.} \end{cases}$$

Comparing Equation (39) with Equation (38), for an infinitely thin aperture, we observe that the difference is compounded in the one-dimensional convolution of the (Fresnel) kernel $\exp(i\alpha y^2)$ with a unit constant of compact support $y \in [-W/2, W/2]$ and the Fourier transform of the same constant (of compact support).

Figure 2 shows example diffraction patterns based on Equations (38) and (39) computed using a uniformly sampled grid of 1000 elements for $y \in [-1, 1]$ with $W = 0.05$ and $k/x = 500$. The results have been obtained using the Matlab functions *fft* (with *fftshift*) and *conv*, to compute the Fourier transform and the convolution operations, respectively. In order to enhance the dynamics of the intensity patterns $I = |A|^2$, the plots are first normalised and plotted on a logarithmic scale given by $\log(0.01 + I/\|I\|_{\infty})$.

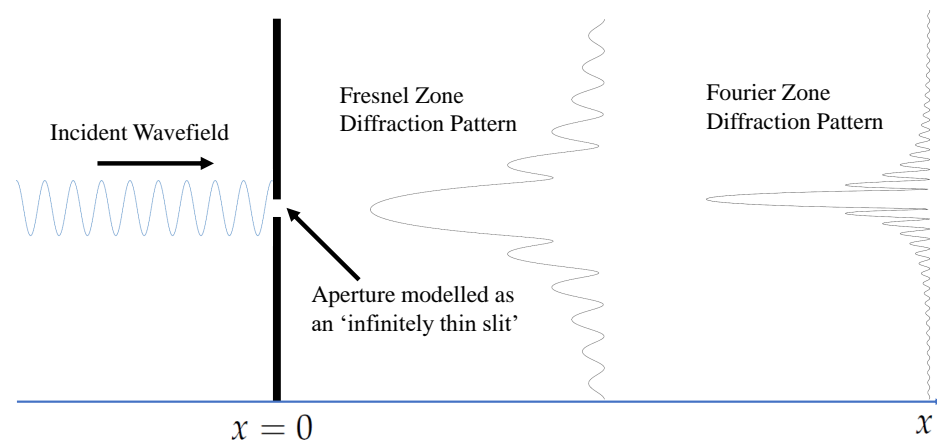


Figure 2. Examples of intensity diffraction patterns given by Equations (38) and (39) in the (two-dimensional) Fresnel and the Fourier zones generated by the scattering of a plane wave propagating through and interacting with a single (infinitely thin) aperture as illustrated—not to scale.

5.3. Fourier and Fresnel Zone Equivalence

Equations (38) and (39) are solutions for the scattering cross-section (the intensity of the scattered wave-field) based on Equation (34) under the conditions that $s/r \ll 1$ and $s^2/r^2 \ll 1$, respectively. Is there a simple relationship between these two results leading to an equivalence principle? The answer to this question involves using the same equivalence relationship for a Fourier transform that was originally designed to develop a fast Fourier transform algorithm by Leo Bluestein in 1970 [32]. It is based on re-writing the discrete Fourier transform in terms of a discrete convolution sum. However, this approach can also be applied for the case of continuous functions as shall now be addressed.

The key to developing the equivalence principle is to note that a Fourier transform (for $\mathbf{r} \in \mathbb{R}^1$) can be written in the form

$$\int_{-\infty}^{\infty} f(x) \exp(-ikx) dx = \exp(-ik^2/2) \int_{-\infty}^{\infty} f(x) \exp(-ix^2/2) \exp[i(k-x)^2/2] dx$$

Thus, using the notation for a convolution integral, we can write Equation (38) in the form

$$|A(K)|^2 = \left| \int_{-\infty}^{\infty} \exp(-iKz) V(z) dz \right|^2 = \left| \exp(iK^2/2) \otimes_K V(K) \exp(-iK^2/2) \right|^2, \quad K = \frac{ky}{x}.$$

Comparing this result with (39), where $\alpha = k/2x$; then, for the case $k/x = 1$, we can construct two equations, namely,

$$|A(y)|^2 = \left| \exp(iy^2/2) \otimes_y V(y) \right|^2 \quad \text{and} \quad |A(y)|^2 = \left| \exp(iy^2/2) \otimes_y V(y) \exp(-iy^2/2) \right|^2$$

for the scattering cross-section in the Fresnel zone and the Fourier zone, respectively.

In the context of these two equations, and, specifically for the case when $k/x = 1$, the difference between the diffraction pattern in the Fresnel zone and the Fourier zone becomes the difference between convolving the chirp function $\exp(iy^2/2)$ with the aperture function $V(y)$ and convolving the same chirp function with the conjugate chirped aperture function $V(y) \exp(-iy^2/2)$.

5.4. Quantification of the Born Approximation

Equations (38) and (39) are effectively the result of considering different geometric scenarios, both of them being taken under the Born approximation—Condition (33). It is therefore worth quantifying this approximation within the context of the model considered for the scattering function, namely, an infinitely thin slit.

For this purpose, we consider the condition using a Euclidean norm for $\mathbf{r} \in \mathbb{R}^2$, i.e., an integrable function $f(\mathbf{r})$ for which we can define

$$\|f(\mathbf{r})\|_2 = \left(\int |f(\mathbf{r})|^2 d^2\mathbf{r} \right)^{\frac{1}{2}}$$

Using inequalities (16), (17) and (18), we can write

$$\|g(r, k) \otimes_{\mathbf{r}} V(\mathbf{r}) U_i(\mathbf{r}, k)\|_2 \leq \|g(r, k)\|_2 \|V(\mathbf{r})\|_2 \|U_i(\mathbf{r}, k)\|_2$$

and Condition (33) therefore becomes

$$\|g(r, k)\|_2 \|V(\mathbf{r})\|_2 \ll 1$$

Given the expression for $g(r, k)$ provided by Equation (32), and, using polar coordinates (r, θ) , $r \in [0, R]$, $\theta \in [0, 2\pi]$, then

$$\|g(r, k)\|_2 = \frac{1}{\sqrt{8\pi k}} \left(\int \frac{d^2\mathbf{r}}{r} \right)^{\frac{1}{2}} = \frac{1}{\sqrt{8\pi k}} \left(\int_0^{2\pi} \int_0^R \frac{r dr d\theta}{r} \right)^{\frac{1}{2}} = \frac{1}{2} \sqrt{\frac{R}{k}}.$$

Thus, defining the root mean square of $V(\mathbf{r})$ as being

$$\bar{V} = \left(\frac{\int |V(\mathbf{r})|^2 d^2\mathbf{r}}{\int d^2\mathbf{r}} \right)^{\frac{1}{2}},$$

the condition for the Born approximation to be valid can be written as

$$\bar{V} \ll \frac{1}{R} \sqrt{\frac{k}{R}} \quad (40)$$

This is the condition for the scattering of a non-relativistic electron or ion beam, quantified by Equation (26). For the case of a beam of photons quantified by Equation (24), the difference is that $V(\mathbf{r})$ is replaced by $-k^2 V(\mathbf{r})$. The condition for the Born approximation to be valid is then given by

$$\bar{V} \ll \frac{1}{(kR)^{\frac{3}{2}}} \quad (41)$$

These conditions have been derived for a disc with radius R , which is a measure of the square root of an area. For an infinitely thin slit of the type illustrated in Figure 2, the area is negligible, and, in this context, both the conditions (40) and (41) are valid. Note, however, that, in the latter case, and, in general, we require that the wavelength λ is significantly larger than the physical dimensions of the scatterer, i.e., for a given value of \bar{V} , we require that $\lambda \gg R$. In other words, for an infinitely thin aperture (or otherwise), the width of the aperture must be small compared to the wavelength in order to generate a diffraction pattern. In the case of Condition (40), $\lambda \ll R^{-3}$.

6. The Electromagnetic Shutter Problem

Having reviewed time-independent scattering for $\mathbf{r} \in \mathbb{R}^2$ under the Born approximation for an infinitely thin aperture, and obtained expressions for the intensity of the diffraction pattern in the plane, we now consider the time-dependent case for $\mathbf{r} \in \mathbb{R}^1$ and

for a scalar EM wave. In this context, the (x, y) plane considered previously is replaced with an (x, t) map. The purpose of this is to emphasise the fact that, while the characteristics of the time-independent diffraction of EM and QM fields are essentially the same, the time-dependent shutter problem is markedly different for the two fields.

With reference to Figure 1, we consider a unit amplitude plane wave that is incident on a shutter, which is opened instantaneously at $t = 0$. The width of the wave-field is taken to be less than the width of the aperture so there are no diffraction effects. In this case, for $c_0 = 1$, Equation (22) becomes

$$\left(\frac{\partial^2}{\partial x^2} - \frac{\partial^2}{\partial t^2} \right) u(x, t) = 0 \quad (42)$$

where $x \in (-\infty, \infty)$, $t \in [0, \infty)$, with initial conditions given by

$$u_0(x) \equiv u(x, 0) = \exp(i\omega x), \text{ and } u_0^{(1)}(x, 0) \equiv \left[\frac{\partial}{\partial t} u(x, t) \right]_{t=0} = 0$$

To solve this problem, we consider the time-dependent Green's function (for $c_0 = 1$). In this case, the Green's function is given by the solution to

$$\left(\frac{\partial^2}{\partial x^2} - \frac{\partial^2}{\partial t^2} \right) G(x | y, t - \tau) = \delta(x - y) \delta(t - \tau) \quad (43)$$

where the notation $G(x | y)$ denotes $G(|x - y|)$.

Time dependent problems of this type require application of the Laplace transform. This is because the (one-sided) Laplace transform is a causal transform and therefore provides the facility to implement initial values for the field $u(x, t)$ and/or its derivative at $t = 0$. Using Relationship (11), Equations (42) and (43) transform to

$$\left(\frac{\partial^2}{\partial x^2} - s^2 \right) \bar{u}(x, s) - su(x, 0) - u^{(1)}(x, 0) = 0 \quad (44)$$

where

$$\bar{u}(x, s) \xleftrightarrow{\mathcal{L}} u(x, t)$$

and

$$\left(\frac{\partial^2}{\partial x^2} - s^2 \right) \bar{G}(x | y, s) - sG(x | y, 0) - G^{(1)}(x | y, 0) = \delta(x - y) \quad (45)$$

where

$$\bar{G}(x | y, s) \xleftrightarrow{\mathcal{L}} G(x | y, t),$$

respectively.

Pre-Multiplying Equation (44) by G and Equation (45) by u , subtracting the results and then integrating over x and t , we can construct a solution for $\bar{u}(x, s)$ given by

$$\bar{u}(x, s) = su(x, 0) \otimes_x \bar{G}(|x|, s) + \left[\bar{u}(x, s) \frac{\partial \bar{G}(|x|, s)}{\partial x} \right]_{-\infty}^{\infty} - \left[\bar{G}(|x|, s) \frac{\partial \bar{u}(x, s)}{\partial x} \right]_{-\infty}^{\infty}$$

for $G(x | y, 0) = 0$ and $G^{(1)}(x | y, 0) = 0$.

The values of $u(x, t)$ and $\partial_x u(x, t)$ at $x = \pm\infty$ are un-specified. Moreover, given that they can be taken to be beyond the spatial domain of interest, they are irrelevant, and can therefore be set to zero. This is consistent with the asymptotic condition that $u(x, t) \rightarrow 0$ as $|x| \rightarrow \infty$. Thus, given the initial condition specified, we can consider the solution

$$\bar{u}(x, s) = u(x, 0) \otimes_x s\bar{G}(|x|, s)$$

Inverse Laplace transforming, and, noting that

$$\frac{\partial}{\partial t} G(|x|, t) \xleftrightarrow{\mathcal{L}} s \bar{G}(|x|, s) - G(|x|, 0),$$

we then obtain the time-dependent solution

$$u(x, t) = u_0(x) \otimes_x \frac{\partial}{\partial t} G(|x|, t) \quad (46)$$

given that $G(|x|, 0) = 0$.

The time-dependent Green's function—the solution to Equation (43)—is given by (for $x > 0$)

$$G(x, t) = \frac{1}{2} H(t - x) - \frac{1}{4}, \text{ where } H(t - x) = \begin{cases} 1, & t - x \geq 0; \\ 0, & t - x < 0. \end{cases}$$

This result can be obtained, by taking the inverse Fourier transform of the time-independent (out-going) Green's function, which, for $\mathbf{r} \in \mathbb{R}^1$, is given by

$$g(x, \omega) = \frac{i}{2\omega} \exp(i\omega |x|)$$

Thus, using Relationship (2), and then applying the convolution theorem,

$$\begin{aligned} G(x, t) &= \frac{1}{4} \frac{1}{2\pi} \int_{-\infty}^{\infty} \frac{2}{i\omega} \exp(i\omega |x|) \exp(i\omega t) dt \\ &= \frac{1}{4} \text{sgn}(t) \otimes_t \delta(t + |x|) = \frac{1}{4} \text{sgn}(t + |x|) \\ &= \frac{1}{2} H(t + |x|) - \frac{1}{4} \end{aligned}$$

Given that, for $x > 0$,

$$\frac{\partial}{\partial t} H(t + x) = \delta(t + x)$$

then, from Equation (46), we have

$$u(x, t) = \frac{1}{2} u_0(x) \otimes_x \delta(t + x) = \frac{1}{2} u_0(x - t) = \frac{1}{2} \exp(i\omega x) \exp(-i\omega t) \quad (47)$$

which describes a wave travelling from left to right (using the quantum mechanical convention [33] in the positive half space of Figure 1).

Figure 3a shows a space-time map of the real component of $u(x, t)$, $x \in [0, 1]$, $t \in [0, 1]$ for $\omega = 20\pi$ computed for a regular grid consisting of $10^3 \times 10^3$ elements and displayed using the Matlab *jet* colour map after normalisation—a map of $\text{Re}[u(x, t)] + 1/2 \in [0, 1]$. Note that the intensity of the field $|u(x, t)|^2$ in this case is a constant $\forall x > 0, t > 0$.

The solution given by Equation (46) is dependent on the initial condition $u_0^{(1)}(x) = 0$. For the case when this condition is non-zero, the equivalent solution is

$$u(x, t) = u_0(x) \otimes_x \frac{\partial}{\partial t} G(|x|, t) + u_0^{(1)}(x) \otimes_x G(|x|, t) \quad (48)$$

For example, if the initial wave function in the negative half-space is

$$u(x, t) = \exp(i\omega x) \exp(-i\omega t),$$

then

$$u_0(x) = \exp(i\omega x), \text{ and } u_0^{(1)}(x) = -i\omega \exp(i\omega x)$$

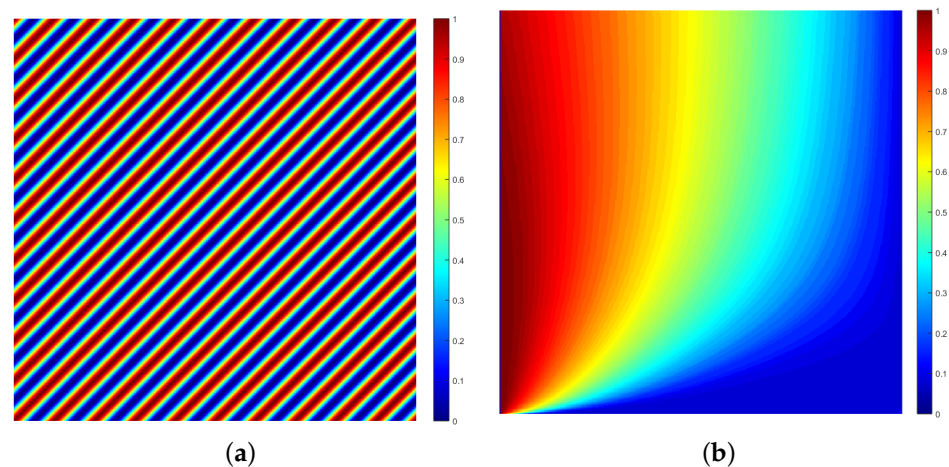


Figure 3. Comparison of the space-time maps for the propagation of photons through an open shutter into a homogenous space (a) and an inhomogeneous space consisting of a complex of random scatterers (b). In both cases, the horizontal axis and the vertical axis, are of space x and time t , respectively, where $(0,0)$ is the lower left-hand corner of the map. (a) space-time map of the real component of the function $u(x,t)$, $x \in [0,1]$, $t \in [0,1]$ given by Equation (47) for $k = \omega = 20\pi$; (b) space-time map of the photon density due to the diffusion of light given by $u(x,t)$ in Equation (57) for $x \in [0,1]$, $t \in [0^+,1]$ with Diffusivity $D = 1$.

7. Multiple Scattering and Diffusion

With reference to Figure 1, the analysis presented so far has assumed that the positive half space is homogenous. The scattering effects are due to an open shutter which yields diffraction patterns as presented in Sections 5.2.1 and 5.2.2 for the time-independent case. This is based on an application of the Born approximation for an aperture that is infinitely thin (when the Born approximation is valid). The shutter problem discussed in Section 6 is illustrative of the fact that, if a beam of photons is incident on a shutter that is instantaneously opened at $t = 0$, then they will simply propagate through the aperture without diffracting, given that the width of the beam is taken to be less than the width of the aperture. This is not the case, when a beam of electrons (or other non-relativistic particles) are incident upon a shutter as will be discussed later. However, before discussing the quantum shutter problem, it is informative to consider the effect of multiple scattering in terms of the physics of diffusion and why this comes about. This is because there is a natural connectivity between this effect and the quantum shutter problem, which relates to the form of the Green's function for the diffusion equation. Furthermore, using this approach provides a way of defining a time-fractional derivative via a memory function which is introduced through a derivation of the Generalised Kolmogorov–Feller Equation as addressed in this section.

7.1. Multiple Scattering

Consider the case when, with reference to Figure 1, the shutter is opened permanently and a beam of photons passes through the aperture without diffracting from the edges as discussed in Section 6. However, the positive half-space is now taken to be composed of a random distribution of scatterers rather than a homogenous free space. In this case, the incident field will interact with a multitude of scatterers, each of them taken to have a physical size of the order of a wavelength. This multiple scattering phenomenon could describe the interaction of photons with water droplets in a fog or a cloud or a turbulent medium, for example. It could also represent the multiple interactions of free electrons in a plasma, for example.

For multiple scattering interactions, the Born approximation is not valid. This is because the Born approximation assumes that only single scattering events occur and that

there are no higher order interactions (double, triple, ..., scattering). Formally, these higher order interactions, relate, respectively, to the terms associated with the iterative solution of Equation (27)—the ‘Born series’—when the scattered is given by:

$$U_s(\mathbf{r}, k) = g(r, k) \otimes_{\mathbf{r}} V(\mathbf{r}) U_i(\mathbf{r}, k) + g(r, k) \otimes_{\mathbf{r}} V(\mathbf{r}) [g(r, k) \otimes_{\mathbf{r}} V(\mathbf{r}) U_i(\mathbf{r}, k)] + \dots \quad (49)$$

The first term on the RHS represents single scattering events (the Born approximation) and the second term represents double scattering events and so on. There are other approaches to modelling a multiple scattered field includes a solution for evaluating the exact scattered field as given in Appendix A. However, if $V(\mathbf{r})$ describes a random ensemble of scatterers, then one can expect the field that evolves to become akin to a process of diffusion where each photon or electron, for example, is taken to undergo a random walk in the plane for $\mathbf{r} \in \mathbb{R}^2$. In addition, this principle is the key to developing a diffusive model for photons (light diffusion) or electron and ion diffusion (which underpins transport theory in a plasma, for example). Modelling multiple scattering as a random walk process requires the problem to be quantified in terms of a time-dependent phenomenon, and, in the following section, the basic field equation—the evolution equation—associated with such a process is addressed.

7.2. The Evolution Equation for a Random Walk

For a canonical ensemble of particles undergoing a random walk involving elastic scattering intersections, the evolution of the density field $u(x, t)$ for $\mathbf{r} \in \mathbb{R}^1$ is given by [34]

$$u(x, t + \tau) = u(x, t) \otimes_x p(x) \quad (50)$$

where $u(x, t)$ is the number of particles per unit length (a real dependent variable where $u(x, t) \geq 0, \forall x, t > 0$) and $p(x)$ is the Probability Density Function (PDF), where

$$\int_{-\infty}^{\infty} p(x) dx = 1 \quad (51)$$

Equation (50) is based on considering how an ensemble of particles introduced at $t = 0$, concentrated solely at a point in space at $x = 0$ becomes distributed over space in a short period of time τ , i.e., if $u(x, 0) = \delta(x)$, then

$$u(x, t) = \delta(x) \otimes_x p(x) = p(x)$$

Thus, $p(x)$ determines how the particles undergoing a random walk are distributed over x in a short period of time t , thereby providing the initial density function $u(x, t)$. As the particles continue to undergo random walks, the density function will continue to evolve in time, subject to the same statistical properties characterised by the PDF. At any future time $t + \tau$, the density function will be determined by the density function at time t convolved with the PDF. This argument is the basis for Equation (50) which is applicable for any PDF. The type of PDF that is considered defines the statistical characteristics of the random walk that occurs, which in turn determines the evolution of the density field.

In terms of the scattering of light, for example, $u(x, t)$ represents the number of photons per unit length (the photon density) at a time t . The density function is equivalent to $|u(x, t)|^2$ in Equation (49) for $\mathbf{r} \in \mathbb{R}^1$ where $u(x, t) \xrightarrow{\mathcal{F}} U(x, k)$, $V(x)$ is replaced by $-k^2 V(x)$ (for the EM case), and where $V(x)$ is a random variable. The incident field at $t = 0$ is not the wave field $u(x, 0)$ but the intensity $|u(x, 0)|^2 = 1$ (for a unit amplitude wave). Thus, with reference to Equation (50), the space-time field $u(x, t)$ must be interpreted in terms of the intensity of a multiple scattered wave field—the scattering cross section for strong scattering interactions leading to an evolution in the spatial distribution of photons.

For quantum scattering (the scattering of electrons in a plasma, for example), $|u(x, t)|^2$ is the probability of a particle existing at a point in space and time, and, in this sense, also represents the electron density, given in Equation (50).

7.2.1. The Evolutionary Equation for $\tau \ll 1$

Applying a Taylor series in time to the function $u(x, t + \tau)$ in Equation (50), then

$$u(x, t + \tau) = u(x, t) + \tau \frac{\partial}{\partial t} u(x, t) + \dots = \sum_{n=0}^{\infty} \frac{\tau^n}{n!} \frac{\partial^n}{\partial t^n} u(x, t)$$

Thus, for $\tau \ll 1$, the evolution equation has the form

$$u(x, t) + \tau \frac{\partial}{\partial t} u(x, t) = u(x, t) \otimes_x p(x) \quad (52)$$

This is known as the Kolmogorov–Feller Equation [35].

7.2.2. The Evolution Equation for a Memory Function

For those cases when we can not assume that $\tau \ll 1$, it is conventional to introduce a ‘memory function’ $m(t)$ by expressing the Taylor series for the function $u(x, t + \tau)$ in Equation (50) as

$$u(x, t + \tau) = \sum_{n=0}^{\infty} \frac{\tau^n}{n!} \frac{\partial^n}{\partial t^n} u(x, t) = u(t) + \tau m(t) \otimes_t \frac{\partial}{\partial t} u(x, t)$$

We can then write the evolution equation in the form

$$u(x, t) + \tau m(t) \otimes_t \frac{\partial}{\partial t} u(x, t) = u(x, t) \otimes_x p(x) \quad (53)$$

This equation is known as the Generalised Kolmogorov–Feller Equation [36].

The reason for using the term ‘memory function’ is that, if $m(t) = \delta(t)$, then Equation (52) is recovered, and, since the delta function is localised entirely at $t = 0$, there is no time memory association in regard to the term $\partial_t u(x, t)$. However, if $m(t) \neq \delta(t)$, then the convolution of $m(t)$ with $\partial_t u(x, t)$ implies that the value of this convolution integral at a time T , say, will depend on the time dependence of $m(t)$, for $t < T$, i.e., the ‘history’ of the function over $t \in [0, T]$. This idea provides an approach to defining a fractional time differential in terms of the convolution of an integer time differential with an appropriate memory function as will be introduced later in Section 9.3.

7.3. The Diffusion Equation

The process of (classical) diffusion can be taken to be the case when $p(x)$ is a normal distribution which, for standard deviation σ , and variance σ^2 , is given by

$$p(x) = \frac{1}{\sigma\sqrt{2\pi}} \exp\left(-\frac{x^2}{2\sigma^2}\right) \xleftrightarrow{\mathcal{F}_1} P(k) = \exp\left(-\frac{\sigma^2 k^2}{2}\right) \sim 1 - \frac{\sigma^2 k^2}{2}, \quad \sigma^2 \ll 1$$

where $P(k)$ is the characteristic function—the Fourier transform of $p(x)$.

In Fourier space, where $u(x, t) \xleftrightarrow{\mathcal{F}_1} U(k, t)$, and, with application of the convolution theorem, we can write Equation (53) as

$$\tau m(t) \otimes_t \frac{\partial}{\partial t} U(k, t) = -\frac{\sigma^2 k^2}{2} U(k, t), \quad \sigma^2 \ll 1$$

which yields the equation, using Relationship (4),

$$m(t) \otimes_t \frac{\partial}{\partial t} u(x, t) = D \frac{\partial^2}{\partial x^2} u(x, t)$$

where D is the ‘Diffusivity’ given by

$$D = \frac{\sigma^2}{2\tau}$$

In this context, the classical diffusion equation

$$\left(D \frac{\partial^2}{\partial x^2} - \frac{\partial}{\partial t} \right) u(x, t) = 0 \quad (54)$$

is recovered when $m(t) = \delta(t)$

In terms of Equation (53), the diffusion equation is a result of considering the case when

$$m(t) = \delta(t) \text{ and } p(x) = \delta(x) + \frac{\sigma^2}{2} \delta^{(2)}(x) \quad (55)$$

where it is noted that

$$\begin{aligned} \int_{-\infty}^{\infty} \delta^{(2)}(x) dx &= \int_{-\infty}^{\infty} dx \frac{d^2}{dx^2} \frac{1}{2\pi} \int_{-\infty}^{\infty} \exp(ikx) dk = \int_{-\infty}^{\infty} dx \frac{1}{2\pi} \int_{-\infty}^{\infty} (-k^2) \exp(ikx) dk \\ &= -\frac{1}{2\pi} \int_{-\infty}^{\infty} dk k^2 \int_{-\infty}^{\infty} \exp(ikx) dx = \int_{-\infty}^{\infty} dk k^2 \delta(k) = 0 \end{aligned}$$

thereby showing that $p(x)$ conforms to Equation (51).

Although we have applied a condition on the variance, it is nevertheless informative to explore the relationship between this measure and the physical nature of a random walk. Within the context of the condition, $\sigma^2 \ll 1$ is used to derive the diffusion equation, and a larger value of σ^2 implies that a particle undergoing a random walk (conforming to a Gaussian distribution) can travel further from the source over a specific period of time. In other words, for a constant value τ , the larger the diffusivity, the greater the range of the random walks so that particles travel further. This implies that the spatial density of scatterers is less so that photons or electrons can diffuse further over the same time interval—the mean free path is greater. This property is compounded in the characteristics of the Green’s function for Equation (54), i.e.,

$$G(x, t) = H(t) \left(\frac{1}{4\pi Dt} \right)^{\frac{1}{2}} \exp \left(-\frac{x^2}{4Dt} \right) \quad (56)$$

where the width of the spatial variance of the exponential function at a given time t is determined by the value of D . This is the same for $\mathbf{r} \in \mathbb{R}^n$ where the Green’s functions have the same basic form, as given by Equation (14).

7.4. Green’s Function Solution to the Diffusion Equation

We apply exactly the same analysis as that given in Section 6 but for Equation (54) instead of Equation (42). This is subject to the initial condition that $u_0(x) \equiv u(x, 0) = 1$, noting that this initial condition is for the intensity of the incident wave field and not the wave field itself, as illustrated in Figure 1. In this case, we obtain the solution

$$u(x, t) = u_0(x) \otimes_x G(x, t) \quad (57)$$

where $G(x, t)$ is given by Equation (56).

This result is obtained by using relationship (11), when, for $D = 1$, Equation (54) and the associated equation for the Green's function, i.e.,

$$\left(\frac{\partial^2}{\partial x^2} - \frac{\partial}{\partial t}\right)G(|x|, t) = \delta(x)\delta(t)$$

transform to

$$\left(\frac{\partial^2}{\partial x^2} - s\right)\bar{u}(x, s) - u(x, 0) = 0 \quad (58)$$

and

$$\left(\frac{\partial^2}{\partial x^2} - s\right)\bar{G}(|x|, s) = \delta(x) \quad (59)$$

respectively. Thus, pre-multiplying these equations by G and u , respectively, subtracting the results and integrating over $x \in (-\infty, \infty)$, we can construct a solution for \bar{u} given by (for $u(x, t) = 0$ and $\partial u(x, t)/\partial x = 0$ at $x = \pm\infty$)

$$\bar{u}(x, s) = u(x, 0) \otimes_x \bar{G}(|x|, s)$$

where $G(x, 0) = 0$. Inverse Laplace transforming then yields Equation (57)

Figure 3b shows a space-time map of $u(x, t)$ for $x \in [0, 1]$, $t \in [0^+, 1]$ (with $D = 1$), computed for a regular grid consisting of $10^3 \times 10^3$ elements and displayed using the Matlab *jet* colourmap after normalisation—a map of $u(x, t)/\|u(x, t)\|_\infty$.

The diffusion of photons or electrons, for example, based on a random walk model in which the 'system' is characterised by a Gaussian PDF, provides a useful background to the (non-relativistic) quantum shutter problem as presented in Section 9. This is essentially because the model used in the analysis of the quantum shutter problem can be said to be based on the diffusion equation for imaginary time, i.e., for $\hbar = 1$ and $m = 1$, then with $D = \frac{1}{2}$ and replacing t with it , Equations (54) and (25) become one and the same (for $\mathbf{r} \in \mathbb{R}^1$). However, before considering this, we formulate and then consider solutions to the space-fractional diffusion equation. This is presented on the following section.

8. Fractional Diffusion

Consider the case when we generalise the Characteristic Function to the form

$$P(k) = \exp(-a |k|^\gamma) \sim 1 - a |k|^\gamma, \quad \gamma \in (1, 2), \quad a < 1$$

where a has the dimensions of $[\text{Length}]^\gamma$ and the index γ is the 'Lévy index'. In this case, the distribution can only be evaluated as an asymptote (at least for $1 < \gamma < 2$) given that

$$\begin{aligned} p(x) &= \mathcal{F}_1^{-1}[\exp(-a |k|^\gamma)] = \mathcal{F}_1^{-1}[1 - a |k|^\gamma + \dots] \\ &= 2\pi\delta(x) - \frac{a}{\Gamma(-\gamma)} |x|^{1+\gamma} + \dots \sim \frac{a}{\Gamma(-\gamma)} |x|^{1+\gamma}, \quad |x| \rightarrow \infty \end{aligned}$$

using Relationship (9).

In the context of the analysis presented in Section 7.3, and, using Relationship (5), the introduction of a Lévy distribution yields the fractional diffusion equation

$$\left(D_\gamma \frac{\partial^\gamma}{\partial |x|^\gamma} - \frac{\partial}{\partial t}\right)u_\gamma(x, t) = 0 \quad (60)$$

where

$$D_\gamma = \frac{a}{\tau}$$

which has dimensions of $[\text{Length}]^\gamma [\text{Time}]^{-1}$. The field $u_\gamma(x, t)$ is used to denote that it is the solution to a fractional differential equation with a spatial differential exponent determined by the value of γ .

In terms of Equation (55), Equation (60) is based on letting

$$m(t) = \delta(t) \text{ and } p(x) = \delta(x) + a\delta^{(\gamma)}(x) \quad (61)$$

8.1. Green's Function for the Space Fractional Diffusion Equation

We now consider the Green's function for the space fractional diffusion operator for $D_\gamma = 1$, which is given by the solution of

$$\left(\frac{\partial^\gamma}{\partial |x|^\gamma} - \frac{\partial}{\partial t} \right) G_\gamma(|x|, t) = -\delta(x)\delta(t), \quad 1 < \gamma < 2 \quad (62)$$

The basis for this is to first of all consider the inter-relationship between the time-independent and time-dependent Green's function for the wave operator and diffusion operator. This is reviewed in the following sections.

8.2. Green's Function for the Wave Operator

We require the solution of

$$\left(\frac{\partial^2}{\partial x^2} - \frac{\partial^2}{\partial t^2} \right) G(|x|, t) = -\delta(x)\delta(t)$$

with

$$G(|x|, t) = \frac{1}{2\pi} \int_{-\infty}^{\infty} g(|x|, \omega) \exp(i\omega t) d\omega \text{ and } \delta(t) = \frac{1}{2\pi} \int_{-\infty}^{\infty} \exp(i\omega t) d\omega,$$

the time-independent form of the problem is given by a solution to the equation

$$\left(\frac{\partial^2}{\partial x^2} + \omega^2 \right) g(|x|, \omega) = -\delta(x)$$

Expressing $g(|x|, \omega)$ in terms of its spatial Fourier transform $\tilde{g}(k, \omega)$, i.e.,

$$g(|x|, \omega) = \frac{1}{2\pi} \int_{-\infty}^{\infty} \tilde{g}(k, \omega) \exp(ik|x|) dk$$

then

$$(-k^2 + \omega^2) \tilde{g}(k, \omega) = -1$$

and

$$g(|x|, \omega) = \frac{1}{2\pi} \int_{-\infty}^{\infty} \frac{\exp(ik|x|) dk}{k^2 - \omega^2} = \frac{1}{2\pi} \int_{-\infty}^{\infty} \frac{\exp(ik|x|) dk}{(k - \omega)(k + \omega)} = \frac{i}{2\omega} \exp(i\omega|x|)$$

This expression arises from an evaluation of an integral which has two poles at $\pm\omega$, the pole for $k = \omega$ providing an expression for the out-going Green's function as given.

8.3. Green's Function for the Classical Diffusion Operator

In the context of evaluating the Green's function for the wave operator discussed in the previous section, suppose we now consider Equation (62) for $\gamma = 2$. In this case, the time-independent Green's function is given by the solution of

$$\left(\frac{\partial^2}{\partial x^2} - i\omega \right) g(|x|, t) = -\delta(x)$$

Applying exactly the same procedure as presented in the previous section, the time-independent Green's function becomes

$$g(|x|, \omega) = \frac{i}{2i\sqrt{i\omega}} \exp[i(i\sqrt{i\omega})|x|] = \frac{1}{2\sqrt{i\omega}} \exp(-\sqrt{i\omega}|x|)$$

This result is based on an evaluation of the integral in the equivalent equation for the Green's function, i.e.,

$$g(|x|, \omega) = \frac{1}{2\pi} \int_{-\infty}^{\infty} \frac{\exp(ik|x|)dk}{(k - i\sqrt{i\omega})(k + i\sqrt{i\omega})}$$

Hence, inverse Fourier transformation, coupled with Relationship (10) yields

$$\begin{aligned} G(|x|, t) &= \frac{1}{2\pi} \int_{-\infty}^{\infty} \frac{1}{2\sqrt{i\omega}} \exp(-\sqrt{i\omega}|x|) \exp(i\omega t) d\omega \\ &= \frac{1}{2\pi i} \int_{0^+ - i\infty}^{0^+ + i\infty} \frac{1}{2\sqrt{s}} \exp(-\sqrt{s}|x|) \exp(st) ds \quad (s = i\omega) \\ &= \frac{1}{2\sqrt{\pi t}} \exp\left(-\frac{|x|^2}{4t}\right), \quad t > 0 \end{aligned}$$

thereby recovering the Green's function for the diffusion equation given by Equation (14) for $\mathbf{r} \in \mathbb{R}^1$ and $D = 1$.

8.4. Green's Functions for the Space Fractional Diffusion Operator

Given the analysis provided in Section 8.3, the time-independent Green's function associated with Equation (62) can be taken to be given by (with $s = i\omega$)

$$g_\gamma(|x|, \omega) = \frac{1}{2s^{\frac{1}{\gamma}}} \exp(-s^{\frac{1}{\gamma}}|x|)$$

which is a generalisation of the result for $\gamma = 2$ to the case when $1 < \gamma < 2$. To implement the inverse Laplace transform required to obtain $G_\gamma(|x|, t)$, we consider a solution under the condition that $|x|^2 \ll 1$ in Laplace space. This condition is analogous to the condition used for developing an expression for the scattering amplitude in the Fresnel zone, as discussed in Section 5.1.2. Thus, we consider a truncated series expression for $g_\gamma(|x|, \omega)$, which is based on the series representation of the exponential function and given by

$$\begin{aligned} g_\gamma(|x|, s) &= \frac{1}{2s^{\frac{1}{\gamma}}} \left(1 - s^{\frac{1}{\gamma}}|x| + \frac{1}{2!} s^{\frac{2}{\gamma}}|x|^2 - \dots \right) \\ &\simeq \frac{1}{2s^{\frac{1}{\gamma}}} - \frac{|x|}{2} + \frac{1}{22!} s^{\frac{1}{\gamma}}|x|^2, \quad |x|^2 \ll 1 \end{aligned}$$

Using Relationships (8) and (9), we can then write

$$\begin{aligned}
 G_{\gamma}(|x|, t) &= \frac{1}{2\Gamma(1/\gamma)t^{1-\frac{1}{\gamma}}} - \frac{|x|\delta(t)}{2} + \frac{|x|^2}{22!\Gamma(-1/\gamma)t^{1+\frac{1}{\gamma}}} \\
 &= \frac{1}{2\Gamma(1/\gamma)t^{1-\frac{1}{\gamma}}} + \frac{|x|^2}{22!\Gamma(-1/\gamma)t^{1+\frac{1}{\gamma}}}, \quad t > 0 \\
 &= \frac{1}{2\Gamma(1/\gamma)t^{1-\frac{1}{\gamma}}} \left(1 + \frac{|x|^2}{2} \frac{\Gamma(1/\gamma)}{\Gamma(-1/\gamma)} \frac{1}{t^{\frac{2}{\gamma}}} \right) \\
 &= \frac{1}{2\Gamma(1/\gamma)t^{1-\frac{1}{\gamma}}} \exp \left(\frac{|x|^2}{2} \frac{\Gamma(1/\gamma)}{\Gamma(-1/\gamma)} \frac{1}{t^{\frac{2}{\gamma}}} \right) \\
 &= \frac{1}{2\Gamma(1/\gamma)t^{1-\frac{1}{\gamma}}} \exp \left(-\frac{|x|^2}{2} \frac{\gamma\Gamma(1/\gamma)}{\Gamma(1-1/\gamma)} \frac{1}{t^{\frac{2}{\gamma}}} \right)
 \end{aligned}$$

where it is noted that

$$\frac{1}{2} \frac{\gamma\Gamma(1/\gamma)}{\Gamma(1-1/\gamma)} \in [0, 1], \quad \gamma \in [1, 2]$$

thereby preserving the negative exponentiation associated with a diffusive process over the range of values for γ considered.

The essential ‘trick’ in developing this expression for $G_{\gamma}(|x|, t)$ is to note that the delta function $\delta(t) = 0, \forall t > 0$, which eliminates the second term, thereby (after factorising) allowing the remaining terms to be recognised as the first two terms in the series definition of an exponential function. This requires that

$$\frac{|x|^2}{2} \frac{\gamma\Gamma(1/\gamma)}{\Gamma(1-1/\gamma)} \frac{1}{t^{\frac{2}{\gamma}}} \ll 1$$

with the upper bound

$$\frac{|x|^2}{2t^{\frac{2}{\gamma}}} < 1 \quad (63)$$

Furthermore, noting that $\Gamma(1/2) = \sqrt{\pi}$, $\Gamma(-1/2) = -2\sqrt{\pi}$, $\Gamma(1) = 1$ and $1/\Gamma(-1) = 0$, we can write, for $t > 0$,

$$G_{\gamma}(|x|, t) = \begin{cases} \frac{1}{2\sqrt{\pi t}} \exp\left(-\frac{|x|^2}{4t}\right), & \gamma = 2; \\ \frac{1}{2}, & \gamma = 1. \end{cases}$$

thereby recovering the expression for the Green’s function when $\gamma = 2$, i.e., Equation (14) for $\mathbf{r} \in \mathbb{R}^1$.

The result for $\gamma = 1$ reflects the Green’s function associated with the operator $\partial_x - \partial_t$, which is given by $\frac{1}{2}H(x - t)$. For completeness, Appendix B considers a similar approach for generating the asymptotic fractional diffusive Green’s function for $\mathbf{r} \in \mathbb{R}^3$; a result that is used later in Section 10.

Repeating the analysis for Equation (60), we obtain

$$G_{\gamma}(|x|, t) = \frac{1}{2D^{\frac{1}{\gamma}}\Gamma(1/\gamma)t^{1-\frac{1}{\gamma}}} \exp \left(-\frac{|x|^2}{2} \frac{\gamma\Gamma(1/\gamma)}{\Gamma(1-1/\gamma)} \frac{1}{D^{\frac{2}{\gamma}}t^{\frac{2}{\gamma}}} \right) \quad (64)$$

8.5. Green's Function Solution to the Space Fractional Diffusion Equation

With the Green's functions for the fractional diffusion operator evaluated for $\mathbf{r} \in \mathbb{R}^1$, and, subject to the initial condition $u_0(x)$, the fractional diffused field, defined by Equation (60), is given by

$$u_\gamma(x, t) = u_0(x) \otimes_x G_\gamma(|x|, t) \quad (65)$$

In reference to Figure 1, the initial condition $u_0(x) = 1, \forall x \leq 0$ represents a constant stream of photons or electrons with a unit density. They then undergo multiple scattering in the positive half space where the multiple scattering is modelled in terms of a space fractional diffusive process; a random walk characterised by a Lévy distribution with a Lévy index between 1 and 2. The field $u(x, t)$ describes the density of photons (the intensity of light) or (non-relativistic) electrons (the number of electrons per unit length) that occurs close to the shutter thereby conforming with the condition that $|x|^2 \ll 1$ to evaluate the Green's function that is used.

An example of the visualisation of the properties associated with Equation (65) is given in Figure 4a. The figure shows a space-time map of $u_\gamma(x, t)$ given by Equation (65) for $\gamma = 1.9$, where $x \in [0, 1], t \in [0^+, 1]$ and $D_\gamma = 1$. The map is computed for a regular grid consisting of $10^3 \times 10^3$ elements and displayed using the Matlab *jet* colour map after normalisation, i.e., a map of $\|u_\gamma(x, t)\|_\infty$, which is visually enhanced using the Matlab function *histeq*. Figure 4b shows a map with exactly the same parameters but for $\gamma = 1.1$. In the former case, and, as expected, the map shows a field that approaches classical diffusion where the density decreases in both space and time. However, for $\gamma \rightarrow 1$, the decay of the field in space becomes increasingly uniform in time. We may consider a demarcation between the values of γ and the type of diffusion that occurs. For $\gamma = 2$, the field is classically diffusive, for $\gamma \in [1, 2)$, the process is sub-diffusive and, for $\gamma < 1$, the process becomes hyper- and super-diffusive.

The methods considered can of course be extended to two- and three-dimensional models. In this respect, the application of space fractional diffusion includes the prediction of market behaviour under the Fractal Market Hypothesis (e.g., [34,37,38]) and the processing and analysis of images [39–41], for example.

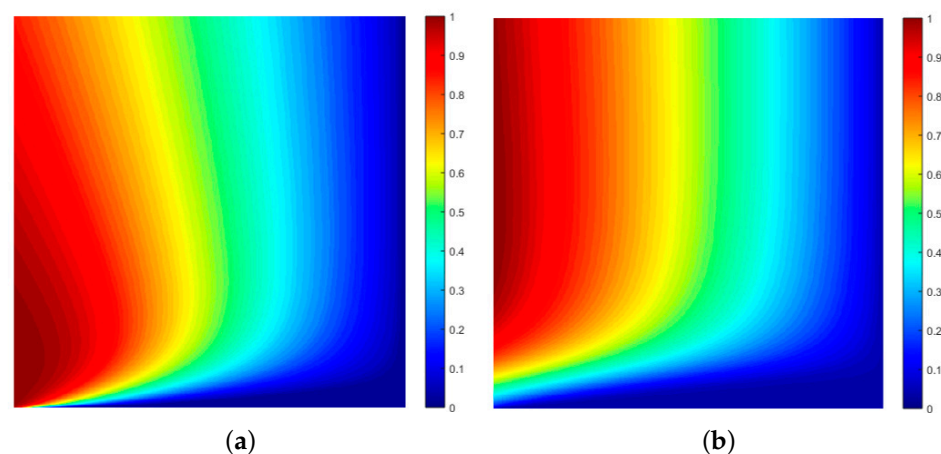


Figure 4. Comparison of the space-time maps for the (space) fractional diffusion of particles interacting with a random medium for $\gamma = 1.9$ (a) and $\gamma = 1.1$ (b). In both cases, the horizontal axis and the vertical axis, are of space x and time t , respectively, where $(0, 0)$ is the lower left-hand corner of the map. (a) Space-time map of the function $u_\gamma(x, t)$ given by Equation (65) for $\gamma = 1.9$; $x \in [0, 1], t \in [0^+, 1]$; (b) space-time map of the function $u_\gamma(x, t)$ given by Equation (65) for $\gamma = 1.1$; $x \in [0, 1], t \in [0^+, 1]$.

9. The Quantum Shutter Problem

As discussed in the Introduction, the ‘quantum shutter’ problem leads to the principle of ‘diffraction in time’ which is a fundamental transient phenomenon in quantum mechanics. In this case, we consider a pencil-line beam of non-relativistic particles described by wave-function $u(x, t)$, which satisfies the time-dependent and one-dimensional Schrödinger’s equation. For $\mathbf{r} \in \mathbb{R}^1$, and, using natural units $m = \hbar = 1$, we are interested in a solution to the equation

$$\left(i \frac{\partial}{\partial t} + \frac{1}{2} \frac{\partial^2}{\partial x^2}\right) u(x, t) = 0 \quad (66)$$

subject to an initial condition $u_0(x) \equiv u(x, t = 0)$.

With references to Figure 1, the initial condition is taken to describe a unit plane wave that is incident upon the shutter before it is instantaneously opened at $t = 0$ and the particle beam is allowed to pass through. The beam is described by a right-traveling unit amplitude plane wave $\exp(ikx)$ which is incident upon a closed shutter placed at $x = 0$.

The shutter is initially taken to be a perfect absorber so that, in the positive half-space, $u(x, t) = 0$, $x > 0$. It is then opened instantaneously at $t = 0$ after which the particle beam is free to travel into the positive half-space. The problem is to find the transient behaviour of the particle beam once it has been made ‘free’ to travel in the positive half-space after the shutter has been opened subject to the initial condition

$$u_0(x) = \begin{cases} \exp(ikx), & x \leq 0; \\ 0, & x > 0. \end{cases} \quad (67)$$

If we consider this problem in regard to the propagation of photons, then the wave function $u(x, t)$, is governed by the classical wave equation as discussed in Section 6. Intuitively, one would consider the photons to propagate into the positive half-space after the shutter is opened so that, for $t > 0$, this half-space is characterised by a linear wave traveling from left to right as verified in the analysis presented in Section 6. However, for a beam on (non-relativistic) electrons, the physical behaviour is entirely different. This is a consequence of the nature of the Green’s function, which, given Equation (14), for $D = 1/2$, $\mathbf{r} \in \mathbb{R}^1$, and imaginary time it becomes

$$G(x, t) = \frac{1}{\sqrt{2\pi it}} \exp\left(\frac{ix^2}{2t}\right), \quad t > 0$$

which is the Green’s function for Equation (66),

Following the approach to generating a Green’s function solution given earlier in the paper, the solution for $u(x, t)$ is given by

$$u(x, t) = G(x, t) \otimes_x u_0(x) \quad (68)$$

illustrating that, like the classical diffusion equation, $u(x, t) \rightarrow 0$ as $t \rightarrow \infty$.

9.1. Solution for the Schrödinger Equation

Compared to a beam of photons, the transient behaviour associated with a beam of electrons, for example (subject to the instantaneous opening of a shutter), is determined by a chirp function. This is a direct consequence of Equation (66) being characterised by the (imaginary) time derivative operator $-i\partial_t$ compared to Equation (22)—for $\mathbf{r} \in \mathbb{R}^1$ —which is characterised by a second order (real) time derivative operator ∂_t^2 . This is also the case for the multi-dimensional Schrödinger equation (for $\hbar = m = 1$)

$$\left(i \frac{\partial}{\partial t} + \frac{1}{2} \nabla^2\right) u(\mathbf{r}, t) = 0, \quad \mathbf{r} \in \mathbb{R}^n$$

given that, from Equation (14), the Green's functions for this case are given by

$$G(\mathbf{r}, t) = \left(\frac{1}{2\pi i t} \right)^{\frac{n}{2}} \exp\left(\frac{i r^2}{2t}\right), \quad t > 0$$

The solution given by Equation (68) can be studied analytically using a change of variables to obtain an expression for the probability density given by [1]

$$|u(x, t)|^2 = \frac{1}{2} \left(\left| C(\xi) + \frac{1}{2} \right|^2 + \left| S(\xi) + \frac{1}{2} \right|^2 \right)$$

where

$$\xi = \frac{(kt - x)}{\sqrt{\pi t}}$$

and $C(\xi)$ and $S(\xi)$ are the Fresnel integrals

$$C(\xi) = \int_0^\xi \cos\left(\frac{\pi u^2}{2}\right) du \quad \text{and} \quad S(\xi) = \int_0^\xi \sin\left(\frac{\pi u^2}{2}\right) du$$

However, Equation (68) can also be computed numerically via application of a convolution sum and the solutions displayed on a space-time map of the type given in Figure 3. Two examples of this are shown in Figure 5, which provides time-diffraction maps of the probability function $|u(x, t)|^2$, where $u(x, t)$ is given by Equation (68). In both cases, the function $|u(x, t)|^2$ is computed on a uniformly sampled grid consisting of $10^3 \times 10^3$ elements and displayed using the Matlab *jet* colour map after normalisation, i.e., a map of $|u(x, t)|^2 \in [0, 1]$. The maps have been enhanced using the Matlab histogram equalisation function *histeq*. They show examples of the oscillations in time (and space) that decay over time and decrease in frequency, the effect being dependent on the value of the wavenumber k associated with the initial condition compounded in Equation (67). As the value of k increases, the oscillatory behaviour 'expands' over the (x, t) plane.

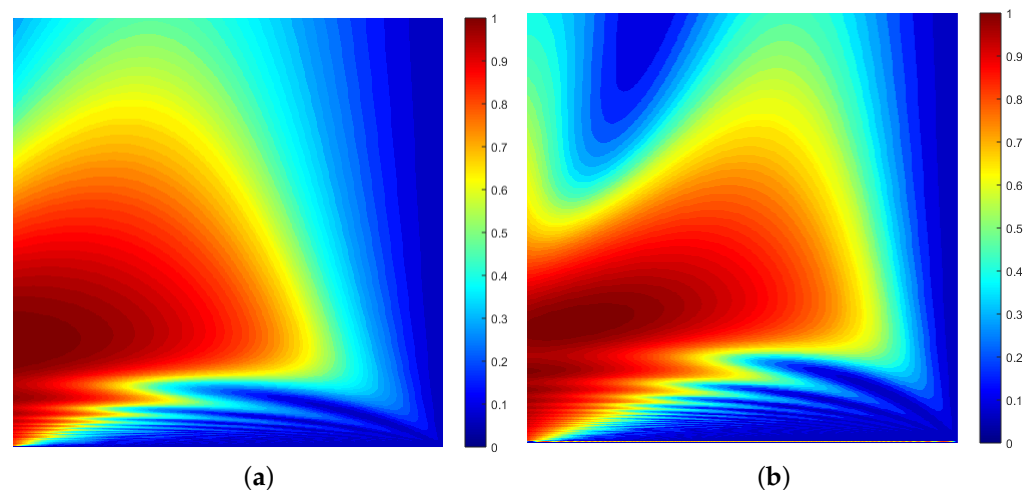


Figure 5. Examples of two time-diffraction maps. In both cases, the horizontal axis and the vertical axis, are of space x and time t , respectively, where $(0, 0)$ is the lower left-hand corner of the map. (a) Space-time map of the function $|u(x, t)|^2$, $x \in [0, 1]$, $t \in [0^+, 1/k]$ where $u(x, t)$ is given by Equation (68) for $k = \pi$; (b) space-time map of the function $|u(x, t)|^2$, $x \in [0, 1]$, $t \in [0^+, 1/k]$ where $u(x, t)$ is given by Equation (68) for $k = 2\pi$.

The examples given in Figure 5 illustrates the oscillatory behaviour and decay of the probability density function for non-relativistic electrons. This is of course very different to the optical case (a beam of photons characterised by the classical wave equation as presented in Section 6) when, by comparison, the intensity function in the positive half-space is a constant, i.e., Figure 3a would be a map of the value 1. There is a similarity between the expression for $u(x, t)$ given by Equation (68) to the Fresnel zone solution given in Equation (39). This is why the transient phenomenon associated with the quantum shutter problem is dubbed ‘diffraction in time’ [1]. It is a quantum effect that requires the application of very low velocity particles, observed over small distances, so that the time interval of an experimental observation is very small, when the Fresnel-type oscillations of the density function in time are prevalent as illustrated in Figure 5.

9.2. Solution for the Space Fractional Schrödinger Equation

In Section 8, the fractional diffusion equation was constructed from Equation (53) on the basis of a delta memory function and a PDF given by $\delta(x) + a\delta(\gamma)$. Suppose we apply the same (phenomenological) principle for constructing the space fractional Schrödinger equation, but for the imaginary memory function $-i\delta(t)$. In this case, because the delta function is imaginary, the field $u(x, t)$ can no longer be taken to be a density function but a complex wave-type function (on a phenomenological basis). In this context, with $a = \eta^\gamma \hbar^2 / (2m)$, where η has dimensions of $[\text{Length}]^\gamma$, and $\tau = \hbar$, we recover the fractional Schrödinger equation (for $\hbar = m = \eta = 1$)

$$\left(\frac{1}{2} \frac{\partial^\gamma}{\partial |x|^\gamma} - \frac{\partial}{\partial(it)} \right) u_\gamma(x, t) = 0 \quad (69)$$

which is an identical equation to Equation (60) for imaginary time it and with $D_\gamma = 1/2$. Thus, we can use the solution given by Equation (65) for the initial condition given by Equation (67), i.e.,

$$u_\gamma(u, t) = u_0(x) \otimes_x G_\gamma(x, t) \quad (70)$$

but where the Green’s function (for $|x|^2 < 1$) is now given by

$$\begin{aligned} G_\gamma(|x|, t) &= \frac{2^{\frac{1}{\gamma}}}{2\Gamma(1/\gamma)(it)^{1-\frac{1}{\gamma}}} \exp\left(-\frac{|x|^2}{2} \frac{\gamma\Gamma(1/\gamma)}{\Gamma(1-1/\gamma)} \frac{2^{\frac{2}{\gamma}}}{(it)^{\frac{2}{\gamma}}}\right) \\ &= \frac{2^{\frac{1}{\gamma}} [\cos(\pi(\gamma-1)/2\gamma) - i \sin(\pi(\gamma-1)/2\gamma)]}{2\Gamma(1/\gamma)t^{1-\frac{1}{\gamma}}} \times \\ &\quad \exp\left[i \sin\left(\frac{\pi}{\gamma}\right) \frac{|x|^2}{2} \frac{\gamma\Gamma(1/\gamma)}{\Gamma(1-1/\gamma)} \frac{2^{\frac{2}{\gamma}}}{t^{\frac{2}{\gamma}}}\right] \exp\left[-\cos\left(\frac{\pi}{\gamma}\right) \frac{|x|^2}{2} \frac{\gamma\Gamma(1/\gamma)}{\Gamma(1-1/\gamma)} \frac{2^{\frac{2}{\gamma}}}{t^{\frac{2}{\gamma}}}\right] \end{aligned}$$

In this case, it is noted that the Green’s function includes an exponential decay which is eliminated as $\gamma \rightarrow 2$ for all values of x and t , conforming to Condition (63), and/or as $t \rightarrow \infty$, $\forall \gamma \in [1, 2]$ and $|x| > 0$.

Two examples of this solution are shown in Figure 6, which provides maps of the probability function $|u_\gamma(x, t)|^2$, where $u_\gamma(x, t)$ is given by Equation (70). The function $|u_\gamma(x, t)|^2$ is computed on a uniformly sample grid consisting of $10^3 \times 10^3$ elements and displayed using the Matlab *jet* colormap after normalisation—a map of $|u_\gamma(x, t)|^2 \in [0, 1]$. The maps have been enhanced using the Matlab histogram equalisation function *histeq*.

These results are illustrative of the fact that, close to the shutter, and, as time increases (after the shutter has been opened), then, for $\gamma \rightarrow 2$, and, for $k = n\pi$, the probability density forms n fringes which decay over time. However, as $\gamma \rightarrow 1$, the decay over time is eliminated, and, consequently, the density function forms a standing fringe pattern that is constant in time. If such a density function could be generated experimentally, then it could form a periodic grating for the diffraction of an electron beam, for example that

is perpendicular to the plane of the grating, for which the diffraction models given in Section 5.2 become relevant.

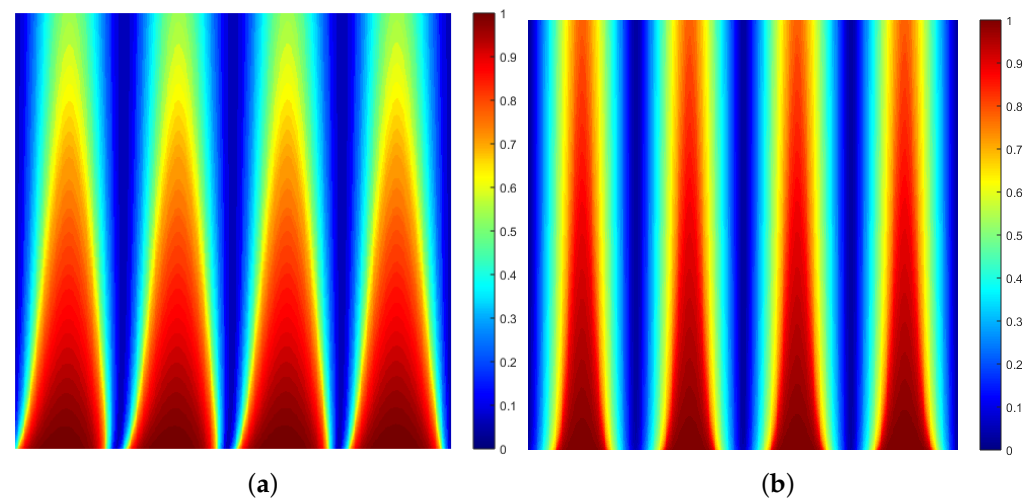


Figure 6. Example of two solutions given by Equation (70). In both cases, the horizontal axis and the vertical axis are of space x and time t , respectively, where $(0,0)$ is the lower left-hand corner of the map. (a) Space-time map of the function $|u_\gamma(x,t)|^2$, $x \in [0,1]$, $t \in [1,k]$ where $u_\gamma(x,t)$ is given by Equation (70) for $k = 4\pi$ and $\gamma = 1.9$; (b) space-time map of the function $|u_\gamma(x,t)|^2$, $x \in [0,1]$, $t \in [1,k]$, where $u_\gamma(x,t)$ is given by Equation (70) for $k = 4\pi$ and $\gamma = 1.1$.

9.3. Time Fractional Solutions

Having discussed the space fractional quantum shutter problem in the previous section, we now consider the time fractional case. This is based on using a memory to represent a fractional time derivative given that $\partial_t^\alpha = \partial_t^{\alpha-1}\partial_t$, $0 < \alpha < 1$. For this range of α , the operator $\partial_t^{\alpha-1}$ is an anti-fractional derivative—a fractional integrator. The most basic fractional integrator is the Riemann–Liouville integral which can be defined as

$$\frac{d^{-\alpha}}{dt^{-\alpha}}f(t) = \frac{1}{\Gamma(\alpha)} \int_0^t \frac{f(x)dx}{(t-x)^{1-\alpha}} \equiv \frac{1}{\Gamma(\alpha)t^{1-\alpha}} \otimes_t f(t)$$

In the context of this definition, and, with respect to Equation (53) with $p(x) = \delta(x) + a\delta^2(x)$, we consider a time fractional diffusion equation given by

$$\tau m_\alpha(t) \otimes_t \frac{\partial}{\partial t} u(x,t) = a \frac{\partial^2}{\partial x^2} u(x,t)$$

where

$$m_\alpha(t) = \frac{1}{\Gamma(1-\alpha)t^\alpha}, \quad 0 < \alpha < 1$$

and it is noted that

$$m_\alpha(t) \otimes_t \frac{\partial}{\partial t} u(x,t) \xleftrightarrow{\mathcal{L}} \frac{1}{s^{1-\alpha}} [s\bar{u}(x,s) - u(x,0)] = s^\alpha \bar{u}(x,s) - \frac{1}{s^{1-\alpha}} u(x,0)$$

However, for $\alpha = 1$, when the classical diffusion equation should be recovered, $1/\Gamma(0) = 0$ and thus

$$m_1(t) \otimes_t \frac{\partial}{\partial t} u(x,t) = 0,$$

a result that is incompatible with the expected limit $\alpha \rightarrow 1$. This incompatibility is due to the fact that the transform

$$\frac{1}{s^\alpha} \xleftrightarrow{\mathcal{L}} \frac{1}{\Gamma(\alpha)t^{1-\alpha}}$$

is strictly only applicable for $\alpha < 1$. Thus, in order to construct a memory function that is compatible with the expected result when $\alpha = 1$, we can define it as

$$m_\alpha(t) = \begin{cases} \frac{1}{\Gamma(1-\alpha)t^\alpha}, & 0 < \alpha < 1; \\ \delta(t), & \alpha = 1. \end{cases}$$

noting that

$$m_0(t) \otimes_t \frac{\partial}{\partial t} u(x, t) = \int_0^t \frac{\partial}{\partial t} u(x, t) dt = u(x, t)$$

9.3.1. Time Fractional Diffusion

Following the approach detailed in Section 7.4, we can now construct a solution for density field $u(x, t)$ given by (for $a/\tau = 1$)

$$u_\alpha(x, t) = m_\alpha(t) \otimes_t G_\alpha(x, t) \otimes_x u_0(x), \quad u_0(x) = 1 \quad (71)$$

where

$$G_\alpha(|x|, t) = \frac{1}{2\Gamma(\alpha/2)t^{1-\frac{\alpha}{2}}} \exp\left(-\frac{|x|^2}{2} \frac{(\alpha/2)\Gamma(\alpha/2)}{\Gamma(1-\alpha/2)} \frac{1}{t^\alpha}\right)$$

Compared to the solution for the space-fractional diffusion equation, the time-fractional case includes a causal convolution in time with the memory function. Furthermore, comparing the fractional indices, it is clear that $1/\gamma = \alpha/2$.

9.3.2. Time Fractional Quantum Shutter

This same principle applies to developing a solution for the time fractional shutter problem. This essentially involves replacing t for it when the solution given by Equation (71)—for the wave function $u(x, t)$ —is given by

$$u_\alpha(x, t) = m_\alpha(t) \otimes_t G_\alpha(x, t) \otimes_x u_0(x), \quad u_0(x) = \exp(ikx), \quad \forall x \leq 0 \quad (72)$$

where

$$m_\alpha(t) = \frac{\exp(-i\pi\alpha/2)}{\Gamma(1-\alpha)t^\alpha}$$

and

$$G_\alpha(|x|, t) = \frac{2^{\frac{\alpha}{2}} [\cos(\pi(2-\alpha)/4) - i \sin(\pi(2-\alpha)/4)]}{2\Gamma(\alpha/2)t^{1-\frac{\alpha}{2}}} \exp\left[i \sin\left(\frac{\pi\alpha}{2}\right) \frac{|x|^2}{2} \frac{(2/\alpha)\Gamma(\alpha/2)}{\Gamma(1-\alpha/2)} \frac{2^\alpha}{t^\alpha}\right] \exp\left[-\cos\left(\frac{\pi\alpha}{2}\right) \frac{|x|^2}{2} \frac{(2/\alpha)\Gamma(\alpha/2)}{\Gamma(1-\alpha/2)} \frac{2^\alpha}{t^\alpha}\right]$$

Two examples of the solution given by Equation (72) are shown in Figure 7, which provides maps of the probability density function $|u_\alpha(x, t)|^2$. As in previous results, the function $|u_\alpha(x, t)|^2$ is computed on a uniformly sample grid consisting of $10^3 \times 10^3$ elements and displayed using the Matlab *jet* colormap after normalisation giving a map of $|u_\alpha(x, t)|^2 \in [0, 1]$, the maps having been enhanced using the Matlab histogram equalisation function *histeq*.

The results illustrated in Figure 7 show that oscillations in time are prevalent when $\alpha \rightarrow 1$ as should be expected, when the solution approaches that of the solution presented in Section 9.1, compounded in Figure 5. However, the time oscillations do not reflect that of a Fresnel diffraction pattern and are of a significantly lower frequency for the same initial condition $u_0(x) = \exp(ikx)$, $\forall x < 0$. On the other hand, as $\alpha \rightarrow 0$, the probability density reflects the standing fringe pattern illustrated in Figure 6, for example, for the space fractional case, but with a greater dissipation in both space and time.

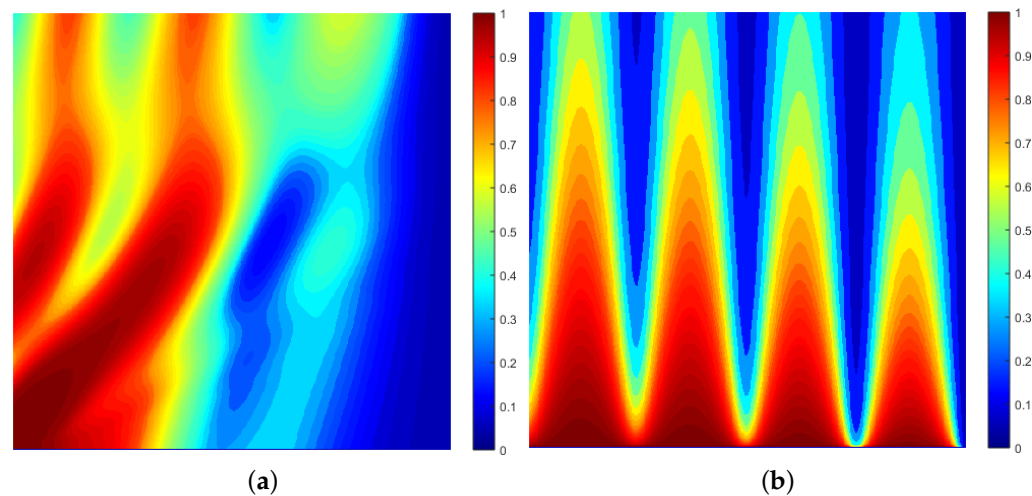


Figure 7. Example of two solutions given by Equation (72). In both cases, the horizontal axis and the vertical axis, are of space x and time t , respectively, where $(0,0)$ is the lower left-hand corner of the map. (a) Space-time map of the function $|u_\alpha(x,t)|^2$, $x \in [0,1]$, $t \in [0^+, 1/k]$ where $u_\alpha(x,t)$ is given by Equation (72) for $k = 4\pi$ and $\alpha = 0.9$; (b) space-time map of the function $|u_\alpha(x,t)|^2$, $x \in [0,1]$, $t \in [0^+, 1/k]$, where $u_\alpha(x,t)$ is given by Equation (72) for $k = 4\pi$ and $\alpha = 0.1$.

10. The Quantum Shutter Problem for the Relativistic and Semi-Relativistic Case

In the final part of this paper, we consider the quantum shutter problem for the relativistic and then the semi-relativistic case. In the latter case, a phenomenological equation is introduced, which is taken to describe a quantum field which is neither non-relativistic or fully-relativistic. In this regard, and, in reference to Figure 1, we consider a beam of ‘semi-relativistic’ particles with velocities of the order of 50–70% light speed. Examples of such particles include the delocalised electrons that exist in Graphene [42]. This is because the charge carriers in Graphene show linear, rather than quadratic, dependence of energy E on momentum p [43,44]. This dependence indicates that they adhere more to the relativistic energy equation $E^2 = p^2 + m^2$ for a charge carrier with mass m (for $\hbar = c_0 = 1$) rather than conforming to the non-relativistic energy equation $E = p^2/2m$.

10.1. Quantum Shutter Problem for the Klein–Gordon Equation

The problem is effectively the same as that considered in Section 9 but instead of solving the problem for the one-dimensional Schrödinger equation, we consider the (one-dimensional) Klein–Gordon Equation given by (for $\hbar = c_0 = m = 1$)

$$\left(\frac{\partial^2}{\partial x^2} - \frac{\partial^2}{\partial t^2} - 1\right)u(x,t) = 0 \quad (73)$$

subject to initial conditions for $u_0(x)$ and $u_0^{(1)}(x)$.

The fundamental solution to this equation is the same as that given by Equation (48), but where the Green’s function is now the solution of

$$\left(\frac{\partial^2}{\partial x^2} - \frac{\partial^2}{\partial t^2} - 1\right)G(|x|,t) = \delta(x)\delta(t)$$

and given by [45]

$$G(|x|,t) = \frac{1}{2}[(1 - \sin t)(\delta(t-x) + \delta(t+x)) + H(t-|x|)J_0(\sqrt{t^2 - x^2})] \quad (74)$$

where J_0 is the Bessel function (of the first kind and of order zero). The fact that this solution depends on a convolution with a Bessel function ensures that the field is characterised by oscillations in both space and time. Two examples of this are given in Figure 8.

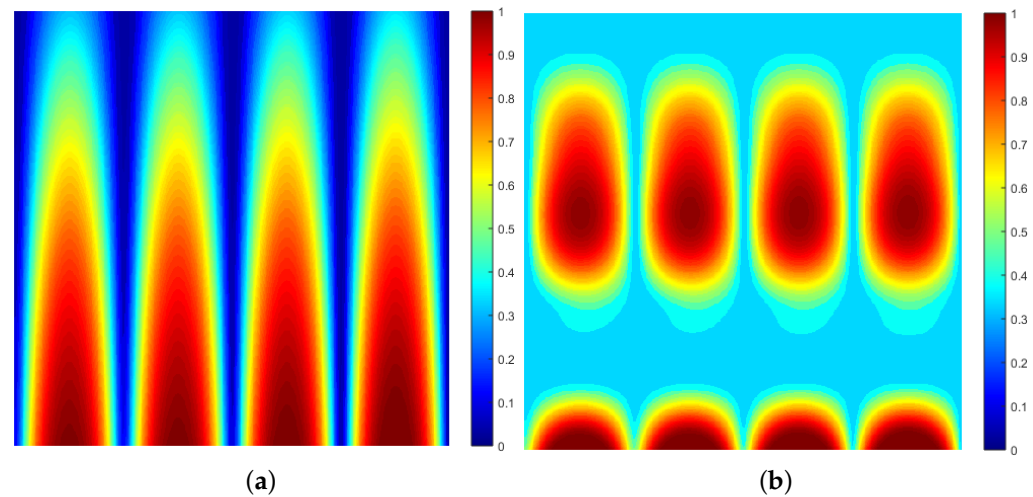


Figure 8. Examples of two solutions of the quantum shutter problem for the Klein–Gordon equation—Equation (73). In both cases, the horizontal axis and the vertical axis are of space x and time t , respectively, where $(0,0)$ is the lower left-hand corner of the map. (a) Space-time map of the function $|u(x,t)|^2$, $x \in [0,1]$, $t \in [0^+, 10/k]$ where $u(x,t)$ is given by Equation (48) for the Green’s function given by Equation (74) for $k = 4\pi$; (b) space-time map of the function $|u(x,t)|^2$, $x \in [0,1]$, $t \in [0^+, 100/k]$ where $u(x,t)$ is given by Equation (48) for the Green’s function given by Equation (74) for $k = 4\pi$.

10.2. Quantum Shutter Problem for the Fractional Klein–Gordon Equation

In the context of the solution to the Klein–Gordon equation considered in the previous section, the following ‘semi-relativistic’ equation is proposed for $0 < \alpha < 1$ where $\xi = -it$ [46]:

$$\left[\left(\frac{1}{2m} \right)^{1-\alpha} \frac{\partial^2}{\partial x^2} + \frac{\partial^{1+\alpha}}{\partial \xi^{1+\alpha}} - \alpha m^2 \right] u(x,t) = 0 \quad (75)$$

$$\Rightarrow \begin{cases} \left(\frac{1}{2m} \frac{\partial^2}{\partial x^2} + i \frac{\partial}{\partial t} \right) u(x,t) = 0, & \alpha = 0; \\ \left(\frac{\partial^2}{\partial x^2} - \frac{\partial^2}{\partial t^2} - m^2 \right) u(x,t) = 0, & \alpha = 1. \end{cases}$$

Equation (75) is an equation for the semi-relativistic field $u(x,t)$, constructed so that it reduces to the homogeneous Schrödinger equation when $\alpha = 0$ and to the Klein–Gordon equation when $\alpha = 1$. Note that Equation (75) is a phenomenology as are the Schrödinger and Klein–Gordon equations. With reference to Figure 1, the aim is to solve Equation (75) for the same initial $u(x,0) = \exp(ikx)$, $\forall x \leq 0$ with $m = 1$, when it can be written in the form

$$\left(\frac{\partial^2}{\partial x^2} + \beta_1 \frac{\partial^\beta}{\partial \xi^\beta} + \beta_2 \right) u_\beta(x,t) = 0$$

where, with $\beta = 1 + \alpha$,

$$\beta_1 = 2^{2-\beta} \text{ and } \beta_2 = (\beta - 1)\beta_1$$

Following the approach presented in Section 9.3, by introducing the memory function

$$m_\beta(\xi) = \frac{\beta_1}{\Gamma(1-\beta)\xi^\beta}, \quad 1 < \beta < 2,$$

we can develop a Green's function solution given by

$$u_\beta(x, \xi) = -m_\beta(\xi) \otimes_\xi G_\beta(x, \xi) \otimes_x u_0(x) \quad (76)$$

where $G_\beta(x, \xi)$ is the solution of

$$\left(\frac{\partial^2}{\partial x^2} + m_\beta(\xi) \otimes_\xi \frac{\partial}{\partial \xi} + \beta_2 \right) G_\beta(x, \xi) = -\delta(x)\delta(\xi)$$

The problem is to evaluate the Green's function for this case, a problem which is now addressed.

Fourier–Laplace transformations allow us to study the Green's function in Fourier–Laplace space, when it can be written as

$$\bar{g}_\beta(k, s) = \frac{1}{k^2 - \Omega^2 - \beta_2} = \frac{1}{k^2 - \Omega^2} \left(1 - \frac{\beta_2}{k^2 - \Omega^2} \right)^{-1} = \frac{1}{k^2 - \Omega^2} \left(1 + \frac{\beta_2}{k^2 - \Omega^2} + \dots \right)$$

where

$$\Omega^2 = \beta_1 s^\beta$$

Inverse Fourier transformation, coupled with application of the convolution theorem, yields

$$\bar{G}_\beta(x, s) = \frac{i}{2\Omega} \exp(i\Omega |x|) + \beta_2 \frac{i}{2\Omega} \exp(i\Omega |x|) \otimes_x \frac{i}{2\Omega} \exp(i\Omega |x|) + \dots$$

The purpose of writing the Green's function in this way is so that one can make use of the property that (using the convolution of two functions application available at [47])

$$\exp(i\Omega |x|) \otimes_x \exp(i\Omega |x|) = \begin{cases} \frac{\exp(i\Omega x)(i+\Omega x)}{\Omega} \simeq x \exp(i\Omega x), & x > 0; \\ \frac{\exp(-i\Omega x)(i-\Omega x)}{\Omega} \simeq -x \exp(-i\Omega x), & x \leq 0, |\Omega| \gg 1. \end{cases}$$

Moreover, using the same application available at [47], it can be shown that

$$\begin{aligned} \exp(i\Omega |x|) \otimes_x [\exp(i\Omega |x|) \otimes_x \exp(i\Omega |x|)] &= \exp(ikx) \frac{(2\Omega^2 x^2 + 2i\Omega x - 1)}{4\Omega^2} \\ &\simeq \exp(ikx) \frac{x^2}{2}, \quad |\Omega| \gg 1. \end{aligned}$$

and similarly that

$$\exp(i\Omega |x|) \otimes_x [\exp(i\Omega |x|) \otimes_x \exp(i\Omega |x|) \otimes_x \exp(i\Omega |x|)] \simeq \exp(ikx) \frac{x^3}{6}$$

so that, in general, for n convolutions, we can write

$$\exp(i\Omega |x|) \otimes_x \dots \otimes_x \exp(i\Omega |x|) \simeq \frac{x^n}{n!} \exp(i\Omega x), \quad |\Omega| \gg 1$$

Thus, through induction, for high frequency fields (which is the case for the semi-relativistic case), we can consider an approximate expression for the Green's function given by (for $|\Omega| \gg 1$)

$$\begin{aligned} \bar{G}_\beta(x, s) &= \frac{i}{2\Omega} \exp(i\Omega x) \left[1 + \frac{i\beta_2 x}{2\Omega} + \frac{1}{2!} \left(\frac{i\beta_2 x}{2\Omega} \right)^2 + \dots \right] \\ &= \frac{i}{2\Omega} \exp(i\Omega x) \exp\left(\frac{i\beta_2 x}{2\Omega}\right), \quad x > 0 \end{aligned}$$

and

$$\begin{aligned}\bar{G}_\beta(x, s) &= \frac{i}{2\Omega} \exp(i\Omega x) \left[1 - \frac{i\beta_2 x}{2\Omega} \exp(-2i\Omega x) + \frac{1}{2!} \left(\frac{i\beta_2 x}{2\Omega} \right)^2 \exp(-2i\Omega x) + \dots \right] \\ &= \frac{i}{2\Omega} \exp(-i\Omega x) \exp\left(-\frac{i\beta_2 x}{2\Omega}\right) + \frac{i}{\Omega} \sin(\Omega x), \quad x \leq 0\end{aligned}$$

Consider the case for $x > 0$. In order to obtain an expression for the time-dependent Green's, we are required to obtain the inverse Laplace transform of $\bar{G}_\beta(x, s)$. The function $i \exp(i\Omega x)/2\Omega$ can be evaluated using the approach taken in Section 9.3. The function $\exp(i\beta_2 x/2\Omega)$ can be evaluated using the same approach as that given in Appendix B. Combining the results, and using the convolution theorem for Laplace transforms, this yields the result

$$\begin{aligned}G_\beta(x, \xi) &= \frac{1}{2\sqrt{\beta_1}\Gamma(\beta/2)\xi^{1-\frac{\beta}{2}}} \exp\left(-\frac{\beta_1 x^2}{4} \frac{\beta\Gamma(\beta/2)}{\Gamma(1-\beta/2)} \frac{1}{\xi^\beta}\right) \\ &\otimes_\xi \frac{i\beta_2}{2\sqrt{\beta_1}} \frac{x}{\Gamma(1-\beta/2)\xi^{1-\beta/2}} \exp\left[-\frac{1}{3!} \left(\frac{\beta_2 x}{2\sqrt{\beta_1}}\right)^2 \frac{\Gamma(\beta/2)}{\Gamma(3\beta/2)} \xi^\beta\right], \quad x > 0\end{aligned}$$

Similarly, for $x \leq 0$,

$$\begin{aligned}G_\beta(x, \xi) &= \frac{1}{2\sqrt{\beta_1}\Gamma(\beta/2)\xi^{1-\frac{\beta}{2}}} \exp\left(-\frac{\beta_1 x^2}{4} \frac{\beta\Gamma(\beta/2)}{\Gamma(1-\beta/2)} \frac{1}{\xi^\beta}\right) \\ &\otimes_\xi \frac{i\beta_2}{2\sqrt{\beta_1}} \frac{-x}{\Gamma(1-\beta/2)\xi^{1-\beta/2}} \exp\left[-\frac{1}{3!} \left(\frac{\beta_2 x}{2\sqrt{\beta_1}}\right)^2 \frac{\Gamma(\beta/2)}{\Gamma(3\beta/2)} \xi^\beta\right] \\ &+ i \left[x + \sum_{n=0}^{\infty} \frac{(-1)^n x^{2n+1}}{(2n+1)!} \frac{\beta_1}{\Gamma(-n\beta)} \frac{1}{\xi^{1+n\beta}} \right]\end{aligned}$$

However, since the inverse Laplace transform is being evaluated for $|x| \ll 1$, the compatible result allows the second term of the Green's function for $x \leq 0$ to be eliminated, leaving the result

$$\begin{aligned}G_\beta(x, \xi) &= \frac{1}{2\sqrt{\beta_1}\Gamma(\beta/2)\xi^{1-\frac{\beta}{2}}} \exp\left(-\frac{\beta_1 x^2}{4} \frac{\beta\Gamma(\beta/2)}{\Gamma(1-\beta/2)} \frac{1}{\xi^\beta}\right) \\ &\otimes_\xi \frac{i\beta_2}{2\sqrt{\beta_1}} \frac{x}{\Gamma(1-\beta/2)\xi^{1-\beta/2}} \exp\left[-\frac{1}{3!} \left(\frac{\beta_2 x}{2\sqrt{\beta_1}}\right)^2 \frac{\Gamma(\beta/2)}{\Gamma(3\beta/2)} \xi^\beta\right], \quad \forall x\end{aligned}$$

Two examples of the solution given by Equation (76) are shown in Figure 9, which provides maps of the probability function $|u_\beta(x, t)|^2$. The maps are computed using a uniformly sample grid consisting of $10^3 \times 10^3$ elements and displayed using the Matlab *jet* colour map after normalisation giving a map of $|u_\beta(x, t)|^2 \in [0, 1]$, both maps having been enhanced using the Matlab histogram equalisation function *histeq*.

Figure 7 implies that, for the semi-relativistic model considered, space-time oscillation is not prevalent for $\alpha \rightarrow 0$, and the probability density decays relatively slowly. However, as $\alpha \rightarrow 1$, the probability density oscillates in space with a period equal to that of the incident wave-field while dissipating in time.

The solution given by Equation (76) implicitly assumes that $u_0^{(1)}(x) = 0$. However, by defining the memory function as

$$m_\alpha(\xi) = \frac{\beta_1}{\Gamma(1-\alpha)\xi^\alpha}, \quad 0 < \alpha < 1$$

the fractional derivative operator $\partial_x^{1+\alpha}$ may be define thus:

$$\frac{\partial^{1+\alpha}}{\partial \xi^{1+\alpha}} \rightarrow m_\alpha(\xi) \otimes_\xi \frac{\partial^2}{\partial \xi^2}$$

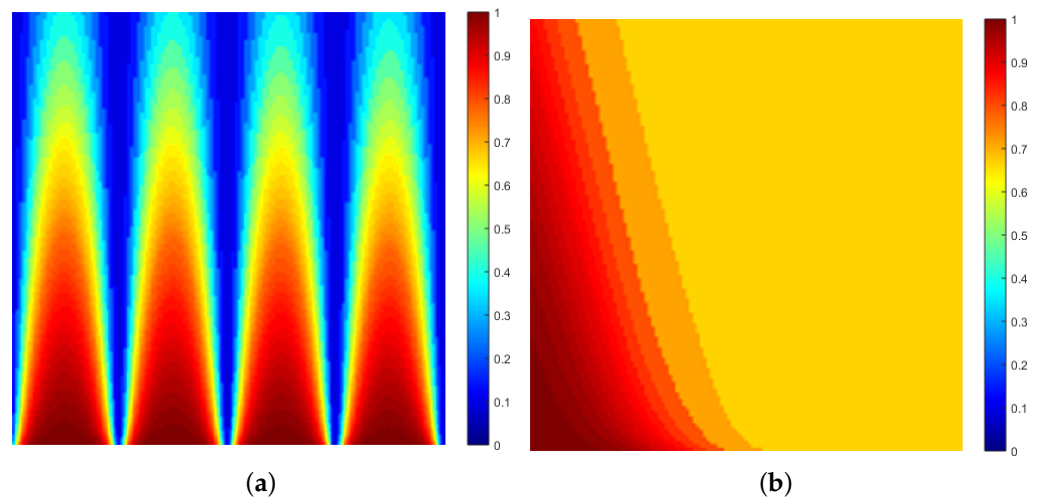


Figure 9. Example of two solutions given by Equation (76). In both cases, the horizontal axis and the vertical axis are of space x and time t , respectively, where $(0,0)$ is the lower left-hand corner of the map. (a) Space-time map of the function $|u_\beta(x,t)|^2$, $x \in [0,1]$, $t \in [0^+, 1/k]$, where $u_\beta(x,t)$ is given by Equation (76) for $k = 4\pi$ and $\alpha = 0.999$; (b) space-time map of the function $|u_\beta(x,t)|^2$, $x \in [0,1]$, $t \in [0^+, 1/k]$, where $u_\beta(x,t)$ is given by Equation (76) for $k = 4\pi$ and $\alpha = 0.001$.

11. Conclusions: Summary and Further Work

Coupled with a review of the more relevant materials, and, coupled with appropriate references, the principal focus of this paper has been to study the quantum shutter problem for fractional quantum fields. In this context, both the space-fractional and time-fractional Schrödinger equations have been considered. Furthermore, the same shutter problem has been considered for a phenomenological equation, which represents the case when the quantum ‘system’ is semi-relativistic.

In all cases, the term ‘shutter problem’ refers to the case when a shutter is opened instantaneously at time $t = 0$, subject to an initial condition $u_0(x) = \exp(ikx)$, $\forall x \leq 0$. The problem is then to evaluate the probability density of the quantum field in the positive half space for all $t > 0$.

11.1. Summary

The study reported in this paper represents an extension of the shutter problem to the field of fractional quantum dynamics. The paper has attempted to explain the models and solutions thereof in terms of a broader connectivity with classical diffraction phenomena and the classical and fractional diffusion equations. This has been done in order to unify the physical models associated with time-independent and then time-dependent phenomena with regard to the interaction of a field with an aperture which is open over all time or opened instantaneously at $t = 0$, respectively.

In order to contextualise the fractional dynamical models considered, the associated non-fractional models and solutions thereof have been presented. This has been done in order to produce an integrated framework, and to provide reference points to prior art. In both cases, the essential key to developing a solution is to evaluate the Green’s functions

for the linear differential operator, fractional or otherwise. Once this function has been evaluated, its convolution with some initial condition provides the basic solution. In this context, the paper has explored solutions to the following:

- The time fractional diffusion equation;
- The space fractional diffusion equation;
- The space fractional Schrödinger equation;
- The time fractional Schrödinger equation;
- The time fractional Klein–Gordon equation.

Example results have been presented to illustrate the behaviour of the solutions as a function of space and time. This has been done by providing enhanced colour maps of the solutions to illustrate the dynamical behaviour of the probability density. In order to provide an example of the Matlab code used to obtain the result presented, Appendix C provides the .m function used to generate the maps given in Figure 5. This function is just one of many that have been generated to output the field maps presented throughout this paper. It is provided as a basic exemplar for the sake of interested readers who may wish to repeat the results given and extend them further.

In the case of the time-fractional problems considered, the issue of defining an initial condition for a fractional time derivative has been addressed through the application of a memory function. Here, a fractional time derivative is represented in terms of a first derivative in time, convolved with the memory function. The memory function is chosen so that application of the Laplace transform yields an expression which incorporates the required initial condition for the field at $t = 0$. This provides an explicit indication of the fact that fractional time derivatives are consistent with modelling a memory associative system.

11.2. Future Work

The analysis presented in this paper has focused on one-dimensional models, providing (x, t) maps to illustrate the one-dimensional dynamical behaviour of the solutions derived. Thus, an obvious extension is to consider the same approach for multi-dimensional models for both space- and time-fractional cases. In this respect, a further, and, more quantitative, analysis is required, based on the methods presented and their extension to multi-dimensional models, subject to a variety of initial conditions. In other words, the results presented are only illustrative examples of a wide range of results that characterise dynamical behaviour based on variations of the fractional exponents γ and α , for the space-fractional and time-fractional derivatives, respectively.

Another area of interest is to compare the multiple scattering solution provided in Appendix A with the time-fractional diffusion equation for the operator $\nabla^2 - \partial_t^{1+\alpha}$, $0 < \alpha < 1$. In principle, this operator describes the intermediate case when scattering interactions are neither fully diffusive ($\alpha = 0$) or fully ‘propagative’ $\alpha = 1$. In this context, such an operator can be used to model a scenario where multiple scattering interactions occur for a limited number of scattering sites; where the density of scatterers reduces to 0 as $\alpha \rightarrow 1$, yielding a model for propagation in a homogeneous half-space. If all scattering sites are taken to be Coulomb potentials, then the results can then be compared directly with the solution given in Appendix A, subject to $\nabla^2 V(\mathbf{r}) = 0$ as discussed in Corollary A2. In this respect, the development of an exact scattering solution for the space fractional Schrödinger equation may be undertaken using a similar approach.

The numerical results presented have been based on the use of a convolution with the corresponding Green's function, a function that, for both space- and time-fractional models, is based on an approximation in which the field is taken to be observed close to the shutter when $|x|^2 < 1$ and where $t \rightarrow 0$. These conditions have been used so that the Green's function has a similar form to the Green's function for the classical diffusion equation. However, there is another approach to developing a numerical evaluation of the fractional quantum fields that can be considered. This is to use the approach presented in Sections 3 and 3.3, given that the Mittag-Leffler function can be computed numerically [30], coupled with the application of an inverse fast Fourier transform.

For the time fractional Schrödinger equation, written in the form

$$\left(i \frac{\partial^2}{\partial x^2} - \frac{\partial^\alpha}{\partial t^\alpha}\right) u(x, t) = 0, \quad u(x, 0) \equiv u_0(x) = \exp(ikx), \quad \forall x \leq 0$$

we can evolve the solution

$$u(x, t) = u_0(x) \otimes_x \frac{1}{2\pi} \int_{-\infty}^{\infty} E_{\alpha,1}(-ik^2 t^\alpha) \exp(ikx) dk$$

This solution may then be investigated by computing the Mittag-Leffler function numerically, applying an inverse fast Fourier transform to the result, and convolving the output with the initial condition.

For the time fractional Klein-Gordon equation considered in Section 10.2, if we consider the equation (where $\beta = 1 + \alpha$)

$$\left[(-i)^\beta \left(\beta_2 + \frac{\partial^2}{\partial x^2}\right) + \beta_1 \frac{\partial^\beta}{\partial t^\beta}\right] u(x, t) = 0$$

subject to the initial conditions $u_0(x)$ and $u_0^{(1)}(x)$, then a solution based on an application of the Mittag-Leffler function can thus be constructed:

$$\begin{aligned} u(x, t) = & u_0(x) \otimes_x \frac{1}{2\pi\beta_1} \int_{-\infty}^{\infty} E_{\alpha,1}[(-i)^\beta \beta_1^{-1} (k^2 - \beta_2) t^\beta] \exp(ikx) dk \\ & + u_0^{(1)}(x) \otimes_x \frac{1}{2\pi\beta_1} \int_{-\infty}^{\infty} E_{\alpha,0}[(-i)^\beta \beta_1^{-1} (k^2 - \beta_2) t^\beta] \exp(ikx) dk \end{aligned}$$

A numerical evaluation of the fractional quantum field can then be investigated by computing the functions $E_{\alpha,1}$ and $E_{\alpha,0}$ numerically [30], applying an inverse fast Fourier transform and convolving the results with the initial condition(s).

Finally, an investigation should be undertaken into the time-fractional Dirac equation for the quantum shutter problem, following the approach taken in [13], for example.

Funding: The research reported in this article was partly funded by the Science Foundation Ireland.

Institutional Review Board Statement: Not applicable.

Informed Consent Statement: Not applicable.

Data Availability Statement: The software developed to present the results given in this work was based solely on the use of Matlab.

Acknowledgments: The author acknowledges the support of the Technological University Dublin, Ireland.

Conflicts of Interest: The author declares no conflict of interest.

Appendix A. Exact Forward and Inverse Schrödinger Scattering Solutions

The results provided in this appendix are based on an attempt to develop an exact solution to the forward and inverse Schrödinger scattering problem.

Statement of the Problem

For $\mathbf{r} \in \mathbb{R}^n$, the solution to the time-independent Schrödinger equation

$$(\nabla^2 + k^2)U(\mathbf{r}, k) = V(\mathbf{r})U(\mathbf{r}, k) \quad (\text{A1})$$

has a fundamental solution given by the Lippmann–Schwinger equation

$$U(\mathbf{r}, k) = U_i(\mathbf{r}, k) + U_s(\mathbf{r}, k) \quad (\text{A2})$$

where u_i is the incident wave function which is taken to be a solution to the equation

$$(\nabla^2 + k^2)U_i(\mathbf{r}, k) = 0 \quad (\text{A3})$$

and $U_s(\mathbf{r}, k)$ is the scattered field given by

$$U_s(\mathbf{r}, k) = g(r, k) \otimes_{\mathbf{r}} V(\mathbf{r})U(\mathbf{r}, k) \quad (\text{A4})$$

where $g(r, k)$ is the free-space and out-going Green's function which is the solution of

$$(\nabla^2 + k^2)g(r, k) = \delta^n(\mathbf{r})$$

On the basis of Equation (A4), the forward scattering problem is 'Given $V(\mathbf{r})$ evaluate $U_s(\mathbf{r}, k)$ '. The corresponding the inverse scattering problem is 'Given $U_s(\mathbf{r}, k)$ evaluate $V(\mathbf{r})$ '. Both problems ideally require unconditional exact solutions.

Theorem A1. *If and only if $(\nabla^2 + k^2)V(\mathbf{r})U_i = 0$ where $(\nabla^2 + k^2)U_i = 0$, then Equation (A4) can be written in the form*

$$U(\mathbf{r}, k) = g(r, k) \otimes_{\mathbf{r}} V(\mathbf{r})U_i(\mathbf{r}, k)$$

where

$$U(\mathbf{r}, k) \xleftrightarrow{\mathcal{F}_n} \frac{\tilde{U}_i(\mathbf{u}, k)\tilde{U}_s(\mathbf{u}, k)}{\tilde{U}_i(\mathbf{u}, k) + \tilde{U}_s(\mathbf{u}, k)}$$

Proof. The key to the proof of this result is to consider the equation

$$V(\mathbf{r})U(\mathbf{r}, k) = W(\mathbf{r}) \otimes_{\mathbf{r}} U(\mathbf{r}, k) \quad (\text{A5})$$

From Equation (A1), and, noting that

$$\nabla^2[W(\mathbf{r}) \otimes_{\mathbf{r}} U(\mathbf{r}, k)] = \nabla^2[W(\mathbf{r})] \otimes_{\mathbf{r}} U(\mathbf{r}, k) = W(\mathbf{r}) \otimes_{\mathbf{r}} \nabla^2 U(\mathbf{r}, k),$$

then

$$\begin{aligned} \nabla^2[V(\mathbf{r})U(\mathbf{r}, k)] &= \nabla^2[W(\mathbf{r}) \otimes_{\mathbf{r}} U(\mathbf{r}, k)] = W(\mathbf{r}) \otimes_{\mathbf{r}} \nabla^2 U(\mathbf{r}, k) \\ &= W(\mathbf{r}) \otimes_{\mathbf{r}} [V(\mathbf{r})U(\mathbf{r}, k) - k^2 U(\mathbf{r}, k)] = W(\mathbf{r}) \otimes_{\mathbf{r}} [W(\mathbf{r}) \otimes_{\mathbf{r}} U(\mathbf{r}, k) - k^2 U(\mathbf{r}, k)] \\ &= W(\mathbf{r}) \otimes_{\mathbf{r}} W(\mathbf{r}) \otimes_{\mathbf{r}} U(\mathbf{r}, k) - k^2 W(\mathbf{r}) \otimes_{\mathbf{r}} U(\mathbf{r}, k) \end{aligned}$$

Thus, introducing the function $\phi(\mathbf{r}, k) = W(\mathbf{r}) \otimes_{\mathbf{r}} U(\mathbf{r}, k)$, Equation (A1) can be written in the form (and without loss of generality)

$$(\nabla^2 + k^2)\phi(\mathbf{r}, k) = W(\mathbf{r}, k) \otimes_{\mathbf{r}} \phi(\mathbf{r}, k)$$

However, this equation has the fundamental solution

$$\phi(\mathbf{r}, k) = \phi_i(\mathbf{r}, k) + g(r, k) \otimes_{\mathbf{r}} W(\mathbf{r}, k) \otimes_{\mathbf{r}} \phi(\mathbf{r}, k) \quad (\text{A6})$$

where $\phi_i(\mathbf{r}, k)$ is taken to be a solution to

$$(\nabla^2 + k^2)\phi_i(\mathbf{r}, k) = 0 \quad (\text{A7})$$

Thus, using the convolution theorem, we can write Equation (A6) for ϕ in \mathbf{u} -space as

$$\tilde{\phi}(\mathbf{u}, k) = \tilde{\phi}_i(\mathbf{u}, k) + \tilde{g}(\mathbf{u}, k) \tilde{W}(\mathbf{u}, k) \tilde{\phi}(\mathbf{u}, k)$$

where $\tilde{\phi}(\mathbf{u}, k)$, $\tilde{g}(\mathbf{u}, k)$ and $\tilde{W}(\mathbf{u}, k)$ are the n -dimensional Fourier transforms of $\phi(\mathbf{r}, k)$, $g(r, k)$ and $W(\mathbf{r}, k)$, respectively. \square

To progress further, we now introduce a crucial condition, which is to let

$$\phi_i(\mathbf{r}, k) = V(\mathbf{r})U_i(\mathbf{r}, k)$$

If we then write this result in terms of $\tilde{U}(\mathbf{u}, k)$, application of the convolution and product theorems yields the Fourier-space equation

$$\frac{1}{(2\pi)^n} \tilde{V}(\mathbf{u}, k) \otimes_{\mathbf{u}} \tilde{U}_i(\mathbf{u}, k) = \tilde{U}(\mathbf{u}, k) \tilde{W}(\mathbf{u}, k) - \tilde{g}(\mathbf{u}, k) \tilde{U}(\mathbf{u}, k) [\tilde{W}(\mathbf{u}, k)]^2 \quad (\text{A8})$$

where $\tilde{V}(\mathbf{u})$ denotes the n -dimensional Fourier transform of $V(\mathbf{r})$, and $\tilde{U}_i(\mathbf{u})$ denotes the n -dimensional Fourier transform of $U_i(\mathbf{r})$. Thus, given Equations (A2) and (A4), we have

$$U(\mathbf{r}, k) = U_i(\mathbf{r}, k) + g(r, k) \otimes_{\mathbf{r}} V(\mathbf{r})U(\mathbf{r}, k)$$

or, given Equation (A5), and, using the convolution theorem

$$\tilde{W}(\mathbf{u}, k) = \frac{\tilde{U}(\mathbf{u}, k) - \tilde{U}_i(\mathbf{u}, k)}{\tilde{g}(\mathbf{u}, k) \tilde{U}(\mathbf{u}, k)}$$

Substituting this expression for $\tilde{W}(\mathbf{u}, k)$ into Equation (A8) and noting that $\tilde{U}(\mathbf{u}, k) - \tilde{U}_i(\mathbf{u}, k) = \tilde{U}_s(\mathbf{u}, k)$, we obtain

$$\frac{\tilde{U}_i(\mathbf{u}, k) \tilde{U}_s(\mathbf{u}, k)}{\tilde{U}_i(\mathbf{u}, k) + \tilde{U}_s(\mathbf{u}, k)} = \frac{1}{(2\pi)^n} \tilde{g}(\mathbf{u}, k) [\tilde{V}(\mathbf{u}, k) \otimes_{\mathbf{u}} \tilde{U}_i(\mathbf{u}, k)]$$

Finally, taking the inverse Fourier transform, we can write this result in the form

$$U(\mathbf{r}, k) = g(r, k) \otimes_{\mathbf{r}} V(\mathbf{r})U_i(\mathbf{r}, k) \quad (\text{A9})$$

where

$$U(\mathbf{r}, k) \xleftrightarrow{\mathcal{F}_n} \frac{\tilde{U}_i(\mathbf{u}, k) \tilde{U}_s(\mathbf{u}, k)}{\tilde{U}_i(\mathbf{u}, k) + \tilde{U}_s(\mathbf{u}, k)} \quad (\text{A10})$$

Corollary A1. From Relationship Equation (A10), it is noted that

$$\frac{\tilde{U}_i(\mathbf{u}, k) \tilde{U}_s(\mathbf{u}, k)}{\tilde{U}_i(\mathbf{u}, k) + \tilde{U}_s(\mathbf{u}, k)} = \frac{\tilde{U}_s(\mathbf{u}, k)}{1 + \frac{\tilde{U}_s(\mathbf{u}, k)}{\tilde{U}_i(\mathbf{u}, k)}} \simeq \tilde{U}_s(\mathbf{u}, k), \quad \frac{\|\tilde{U}_s(\mathbf{u}, k)\|}{\|\tilde{U}_i(\mathbf{u}, k)\|} \ll 1$$

Thus, Relationship (A10) is reduced to

$$U(\mathbf{r}, k) \xleftrightarrow{\mathcal{F}_n} \tilde{U}_s(\mathbf{u}, k)$$

and Equation (A9) becomes

$$U_s^B(\mathbf{r}, k) = g(r, k) \otimes_{\mathbf{r}} V(\mathbf{r}) U_i(\mathbf{r}, k) \quad (\text{A11})$$

where $U_s^B(\mathbf{r}, k)$ is the scattered field under the condition applied.

This result is equivalent to the Born approximation discussed in Section 5.1, i.e., Equation (34) under condition Equation (33). The exact scattering solution given by Equation (A9) therefore reduces to the Born approximation under the condition that the scattered field is much weaker than the incident field.

Corollary A2. Equation (A9) depends explicitly on the condition that

$$(\nabla^2 + k^2)V(\mathbf{r})U_i(\mathbf{r}, k) = 0 \quad (\text{A12})$$

Coupled with the condition that $(\nabla^2 + k^2)U_i(\mathbf{r}, k) = 0$, it is therefore imperative that we consider the ramifications of this condition on the solution developed—in other words, what are the scattering potentials $V(\mathbf{r})$ for which Equation (A12) is applicable.

The first approach for doing this is to expand Equation (A12) and write it in the form

$$\nabla^2 V(\mathbf{r}) + 2\nabla V(\mathbf{r}) \cdot \nabla \ln U_i(\mathbf{r}, k) = 0$$

It is then apparent that, for any incident plane wave-field $U_i(\mathbf{r}, k) = \exp(\pm i\mathbf{k} \cdot \mathbf{r})$ with a constant amplitude A or amplitude spectrum $A(k)$, we can write

$$\nabla^2 V(\mathbf{r}) \pm 2i\mathbf{k} \cdot \nabla V(\mathbf{r}) = 0 \quad (\text{A13})$$

which has the general solution (for arbitrary constants C_1 and C_2)

$$V(\mathbf{r}) = C_1 \exp(\mp 2i\mathbf{k} \cdot \mathbf{r}) + C_2$$

Thus, one condition on the scattering potential is that it is a plane wave oscillating at twice the frequency of the incident plane wave. However, if the potential is taken to be real only, then Equation (A13) suggests that the scattering potential is constrained to satisfying the Laplace equation, i.e.,

$$\nabla^2 V(\mathbf{r}) = 0 \quad (\text{A14})$$

This allows us to consider the Coulomb potential for a point charge (ignoring any scaling constant)

$$V(\mathbf{r}) = \frac{1}{r}, \quad r > 0$$

However, this condition on the scattering function also allows for the sum of such potentials to be considered, when

$$V(\mathbf{r}) = \sum_{n=1}^{\infty} \frac{1}{|\mathbf{r} - \mathbf{r}_n|}, \quad \mathbf{r} \neq \mathbf{r}_n$$

and where the position vector at which the multiple potentials occur can be regular or random. Thus, the exact scattering solution may, in principle, be applied to a medium consisting of a random distribution of point charges such as a plasma—electrons scattering from electrons.

Other potentials $V(\mathbf{r})$ that satisfy Equation (A14) are available depending on the dimension of $\mathbf{r} \in \mathbb{R}^n$. This includes the harmonic functions and their linear combination. For a potential of compact support, the boundary conditions for which a solution to Equation (A14) is required need to be compatible with those that provide a solution for

$U(\mathbf{r}, k)$ which conforms to Equation (A2). These conditions include $U(\mathbf{r}, k) = U_i(\mathbf{r}, k)$ and $\nabla U(\mathbf{r}, k) = \nabla U_i(\mathbf{r}, k)$ on the surface of $V(\mathbf{r})$.

Corollary A3. The condition on the scattering potential can be investigated further on the basis of convolving Equation (A12) with the free-space Green's function when we can write

$$\begin{aligned} g(r, k) \otimes_{\mathbf{r}} \nabla^2 [V(\mathbf{r}) U_i(\mathbf{r})] + k^2 g(r, k) \otimes_{\mathbf{r}} V(\mathbf{r}) U_i(\mathbf{r}) \\ = g(r, k) \otimes_{\mathbf{r}} \nabla^2 [V(\mathbf{r}) U_i(\mathbf{r})] + k^2 U(\mathbf{r}, k) = 0 \end{aligned}$$

where $U(\mathbf{r}, k)$ is given by Equation (A9) from which the exact scattered field $U_s(\mathbf{r}, k)$ can be evaluated. Fourier transformation then yields the \mathbf{u} -space equation

$$\frac{-u^2}{u^2 - k^2} \frac{1}{(2\pi)^n} [\tilde{V}(\mathbf{u}) \otimes_{\mathbf{u}} \tilde{U}_i(\mathbf{u}, k)] = -k^2 \tilde{U}(\mathbf{u}, k) \quad (\text{A15})$$

so that, upon rearrangement and inverse transformation, we can write

$$\begin{aligned} V(\mathbf{r}) &= \frac{k^2 U_i^*(\mathbf{r}, k)}{|U_i(\mathbf{r}, k)|^2} [U(\mathbf{r}, k) + k^2 h(\mathbf{r}) \otimes_{\mathbf{r}} U(\mathbf{r}, k)], \quad h(\mathbf{r}) \leftrightarrow -\frac{1}{u^2} \\ &= k^2 U_i^*(\mathbf{r}, k) [U(\mathbf{r}, k) + k^2 h(\mathbf{r}) \otimes_{\mathbf{r}} U(\mathbf{r}, k)], \quad U_i(\mathbf{r}, k) = \exp(\pm i\mathbf{k} \cdot \mathbf{r}) \end{aligned}$$

which provides an exact inverse scattering solution.

The function $h(\mathbf{r})$ depends on the dimensionality of the solution that is required, and is given by the following: For $\mathbf{r} \in \mathbb{R}^n$, and, $r \equiv |\mathbf{r}|$,

$$h(\mathbf{r}) = \begin{cases} \frac{x}{2} \operatorname{sgn}(x), & n = 1; \\ \frac{1}{2\pi} \ln r, & n = 2; \\ -\frac{1}{4\pi r}, & n = 3. \end{cases}$$

These functions are the Green's function for the Laplace equation, i.e., solutions to the equation

$$\nabla^2 h(r) = \delta^n(\mathbf{r})$$

Remark A1. In terms of using Theorem A1 to compute the exact scattered field, for potentials that conform to those presented in Corollary A2, the exact scattered field is computed through application of Equation (A9) directly. For scattering functions $V(\mathbf{r})$ that do not conform to the conditions presented in Corollary A2, then, from Equation (A15) and Relationship (A10), we can construct an expression for the Fourier transform of the scattered field given by

$$\tilde{U}_s(\mathbf{u}, k) = \frac{u^2 \tilde{U}_i(\mathbf{u}, k) [\tilde{V}(\mathbf{u}) \otimes_{\mathbf{u}} \tilde{U}_i(\mathbf{u}, k)]}{(2\pi)^n k^2 (u^2 - k^2 \pm i\epsilon) U_i(\mathbf{u}, k) - u^2 [\tilde{V}(\mathbf{u}) \otimes_{\mathbf{u}} \tilde{U}_i(\mathbf{u}, k)]}, \quad \epsilon \rightarrow 0$$

We can then consider the asymptotic solution

$$U_s(\mathbf{r}, k) \sim -\frac{1}{k^2} g(r, k) \otimes_{\mathbf{r}} \nabla^2 [V(\mathbf{r}) U_i(\mathbf{r}, k)], \quad k \rightarrow \infty$$

Appendix B. Fractional Diffusive Green's Functions for $\mathbf{r} \in \mathbb{R}^3$

For $\mathbf{r} \in \mathbb{R}^3$, we use the Green's function for $n = 3$ as given in Equation (15) and consider the expansion, for $r^2 \ll 1$,

$$G_\gamma(\mathbf{r}, s) \simeq \frac{1}{4\pi r} \exp(-s^{\frac{1}{\gamma}} r) = \frac{1}{4\pi} \left(\frac{1}{r} - s^{\frac{1}{\gamma}} + \frac{1}{2!} s^{\frac{2}{\gamma}} r - \frac{1}{3!} s^{\frac{3}{\gamma}} r^2 \right)$$

Using Equations (8) and (9), we can then write

$$\begin{aligned} G_\gamma(\mathbf{r}, t) &= \frac{1}{4\pi} \left(\frac{\delta(t)}{r} - \frac{1}{\Gamma(-1/\gamma)} \frac{1}{t^{1+\frac{1}{\gamma}}} + \frac{r}{2!} \frac{1}{\Gamma(-2/\gamma)} \frac{1}{t^{1+\frac{2}{\gamma}}} - \frac{r^2}{3!} \frac{1}{\Gamma(-3/\gamma)} \frac{1}{t^{1+\frac{3}{\gamma}}} \right) \\ &= -\frac{1}{4\pi} \frac{1}{\Gamma(-1/\gamma)} \frac{1}{t^{1+\frac{1}{\gamma}}} \left(1 - \frac{r}{2!} \frac{\Gamma(-1/\gamma)}{\Gamma(-2/\gamma)} \frac{1}{t^{\frac{1}{\gamma}}} + \frac{r^2}{3!} \frac{\Gamma(-1/\gamma)}{\Gamma(-3/\gamma)} \frac{1}{t^{\frac{2}{\gamma}}} \right), \quad t > 0 \\ &\simeq -\frac{1}{4\pi} \frac{1}{\Gamma(-1/\gamma)} \frac{1}{t^{1+\frac{1}{\gamma}}} \left(1 + \frac{r^2}{3!} \frac{\Gamma(-1/\gamma)}{\Gamma(-3/\gamma)} \frac{1}{t^{\frac{2}{\gamma}}} \right), \quad t \rightarrow 0 \\ &\sim \frac{1}{4\pi} \frac{1}{\gamma \Gamma(1-1/\gamma)} \frac{1}{t^{1+\frac{1}{\gamma}}} \exp \left(-\frac{r^2}{3!} \frac{\gamma \Gamma(1-1/\gamma)}{\Gamma(-3/\gamma)} \frac{1}{t^{\frac{2}{\gamma}}} \right) \end{aligned}$$

Noting that $\Gamma(1-1/2) = \sqrt{\pi}$ and $\Gamma(-3/2) = 4\sqrt{\pi}/3$,

$$G_2(\mathbf{r}, t) = \frac{1}{8\pi\sqrt{\pi}t^{\frac{3}{2}}} \exp \left(-\frac{r^2}{4t} \right)$$

thereby recovering the expression for the Green's function for the case of classical diffusion for $\mathbf{r} \in \mathbb{R}^3$ when $\gamma = 2$, i.e., Equation (14). For $\mathbf{r} \in \mathbb{R}^1$, $G_{\gamma \in [1,2]}(\mathbf{r}, t)$ is characterised by a negative exponential $\forall \gamma \in [1,2]$, whereas, for $\mathbf{r} \in \mathbb{R}^3$, $G_{\gamma \in [1,2]}(\mathbf{r}, t)$ changes from a negative exponential for $\gamma > 3/2$ to a positive exponential for $\gamma < 3/2$, and, $G_{3/2}(\mathbf{r}, t)$ scales as $1/t^{5/3}$.

Appendix C. Example Matlab Function

The Matlab function provided in this Appendix is given as an exemplar for interested readers who wish to repeat the results presented in the paper and extend them further. The function specifically relates to the maps provided in Figure 5 with regard to the quantum shutter problem, originally addressed in [1], is discussed in Section 9. The results given in Figure 5 (images (a) and (b), respectively) are obtained by executing the functions

```
QS(1000,pi)
```

and

```
QS(1000,2*pi)
```

```
function QS(n,k)
```

```
%
```

```
%FUNCTION:
```

```
%Evaluates the space-time probability density function associated with the  
%Quantum Shutter (QS) problem discussed in Section 9 and displays the  
%result using the enhanced Matlab colour map 'jet'.
```

```
%
```

```
%INPUTS:
```

```
%n - size of the space-time array (n x n).
```

```
%k - value of the wave-number (typically a multiple of pi).
```

```
%
```

```
%Compute the initial condition in the negative half-space.
```

```

for i=1:floor(n/2)
    x=(i-floor(n/2))/(n/2);
    u_0(i)=exp(1i*2*k*x);
end
%Compute the initial condition for the positive half-space.
for i=floor(n/2)+1:n
    u_0(i)=0;
end
%Start process (j counter for time t and i counter for space x).
for j=1:n/2
    t=j/(k*n/2);
    for i=1:n
        x=(i-floor(n/2))/(n/2);
%Compute the Green's function
        G(i,j)=exp(-(x*x)/(2*(1i*t)))/(2*sqrt(1i*pi*t));
    end
%Evaluate the kernel K for repeated space convolution.
    for i=1:n
        K(i)=G(i,j);
    end
%Convolve the arrays (i.e., the initial condition with the
%Green's function), returning the central component of
%the convolution that is the same size as the kernel.
    c=conv(u_0,K,'same');
%Compute the (space-time) wave function.
    for i=1:n
        u(i,j)=c(i);
    end
end
%Compute the probability density in the positive half-space only.
for j=1:n/2
    for i=1:n/2
        I(i,j)=abs(u(i+n/2-1,j)).^2;
    end
end
%Normalise and enhance the output image using
%histogram equalisation.
I=I./max(max(abs(I))); I=histeq(I);
%Rotate the image so that the horizontal axis defines space
%and the vertical axis defines time.
I = imrotate(I,90);
%Apply the colour map 'jet'.
myColorMap = jet(256);
%Display the image in Figure 1 together with the colorbar.
figure(1), imshow(I, 'Colormap', myColorMap); colorbar

```

References

1. Moshinsky, M. Diffraction in Time. *Phys. Rev.* **1952**, *88*, 625–631. [[CrossRef](#)]
2. Evans, G.; Blackledge, J.M.; Yardley, P. *Analytic Solutions to Partial Differential Equations*; Springer: London, UK, 1999; ISBN 2540761241.
3. Blackledge, J.M. *Digital Image Processing: Mathematical and Computational Methods*; Woodhead Publishing Series in Electronic and Optical Materials: Amsterdam, The Netherlands, 2005. Available online: <https://arrow.tudublin.ie/engschelebk/3/> (accessed on 4 January 2022).
4. Blackledge, J.M. On the Chirp Function, the Chirplet Transform and the Optimal Communication of Information. *IAENG Int. J. Appl. Math.* **2020**, *50*, 285–319.

5. Goussev, A. Diffraction in Time: An Exactly Solvable Model. *Phys. Rev. A* **2013**, *87*, 1–5. [CrossRef]
6. Brukner, C.; Zeilinger, C. Diffraction of Matter Waves in Space and in Time. *Phys. Rev. A* **1997**, *56*, 3804–3824. [CrossRef]
7. Kleber, M. Exact Solutions for Time-dependent Phenomena in Quantum Mechanics. *Phys. Rep.* **1994**, *236*, 331–393. [CrossRef]
8. del Campo, A.; Garcia-Calderon, G.; Mugar, J.G. Quantum Transients. *Phys. Rep.* **2009**, *476*, 1–50. [CrossRef]
9. Szriftgiser, P.; Guéry-Odelin, D.; Arndt, M.; Dalibard, J. Atomic Wave Diffraction and Interference Using Temporal Slits. *Phys. Rev. Lett.* **1996**, *77*, 4–7. [CrossRef]
10. Beau, M.; Dorlas, T.C. Three-dimensional Quantum Slit Diffraction and Diffraction in Time. *Dublin Inst. Adv. Stud.* **1996**, *54*, 1882–1907. [CrossRef]
11. Umil, Y.Z. General Formulation of the Scattered Matter Waves by a Quantum Shutter. *Turk. J. Phys.* **2008**, *33*, 1–9.
12. Bindel, L. A New Theory of Diffraction in Time. *ResearchGate* **2018**. Available online: https://www.researchgate.net/publication/323784268_A_NEW_THEORY_OF_DIFFRACTION_IN_TIME (accessed on 2 March 2022).
13. Godoy, S.; Villa, K. A Basis for Causal Scattering Waves, Relativistic Diffraction in Time Functions. *J. Mod. Phys.* **2016**, *7*, 1181–1191. [CrossRef]
14. Mainardi, F. Fractional Calculus: Theory and Applications. *J. Math.* **2018**, *6*, 145. [CrossRef]
15. Laskin, N. *Fractional Quantum Mechanics*; World Scientific Publishing: Singapore, 2018; ISBN 978-981-3223-79-0. [CrossRef]
16. Iomin, A. Fractional Evolution in Quantum Mechanics. *Chaos Solitons Fractals* **2019**, *1*, 100001. [CrossRef]
17. Nasrolahpour, H. Time Fractional Formalism: Classical and Quantum Phenomena. 2012. Available online: <https://arxiv.org/ftp/arxiv/papers/1203/1203.4515.pdf> (accessed on 25 February 2022).
18. Gorenflo, R.; Kilbas, A.A.; Mainardi, F.; Rogosin, S.V. *Mittag–Leffler Functions, Related Topics and Applications*; Springer: New York, NY, USA, 2014; ISBN 978-3-662-43929-6.
19. Apelblat, A. Differentiation of the Mittag–Leffler Functions with Respect to Parameters in the Laplace Transform Approach. *J. Math.* **2020**, *8*, 657. [CrossRef]
20. Garrappa, R. Numerical Solution of Fractional Differential Equations: A Survey and a Software Tutorial. *J. Math.* **2018**, *6*, 16. [CrossRef]
21. WolframAlpha. Fourier Transform Calculator. 2022. Available online: <https://www.wolframalpha.com/input/?i=Fourier+transform+calculator> (accessed on 16 January 2022).
22. Schiff, J.L. *The Laplace Transform: Theory and Applications*; Springer: New York, NY, USA, 1999; ISBN-10 0387986987.
23. WolframAlpha. Laplace Transform Calculator. 2022. Available online: <https://www.wolframalpha.com/input/?i=laplace+transform> (accessed on 25 January 2022).
24. Liang, S.; Wu, R.; Chen, L. Laplace Transform of Fractional Order Differential Equations. *Electron. J. Differ. Equat.* **2015**, *2015*, 1–15.
25. Blackledge, J.M. A New Definition, a Generalisation and an Approximation for a Fractional Derivative with Applications to Stochastic Time Series Modeling. *IAENG Eng. Lett.* **2021**, *29*, 138–150.
26. Valerio, D.; Ortigueira, M.D.; Lopes, A.M. How Many Fractional Derivatives Are There? *J. Math.* **2022**, *10*, 737. [CrossRef]
27. Mainardi, F. The Fundamental Solutions for the Fractional Diffusion-wave Equation. *Appl. Math. Lett.* **1996**, *9*, 23–28. [CrossRef]
28. Paneva-Konoska, J. Series in Mittag–Leffler Functions. *Adv. Math. Sci. J.* **2021**, *2*, 73–79.
29. Achar, B.N.N.; Yale, B.T.; Hanneken, J.W. Time Fractional Schrödinger Equation Revisited. *Adv. Math. Phys.* **2013**, *2013*, 1–11. [CrossRef]
30. Podlubny, I. Mittag–Leffler Function. 2022. Available online: <https://www.mathworks.com/matlabcentral/fileexchange/8738-mittag-leffler-function> (accessed on 3 February 2022).
31. Lipnevicha, V.; Luchkob, Y. The Wright Function: Its Properties, Applications, and Numerical Evaluation. In *AIP Conference Proceedings*; American Institute of Physics: College Park, MD, USA, 2010; Volume 1301. [CrossRef]
32. Bluestein, L. A Linear Filtering Approach to the Computation of Discrete Fourier Transform. *IEEE Trans. Audio Electroacoust.* **1970**, *18*, 451–455. [CrossRef]
33. Jones, J.A. Wave Conventions: The Good, the Bad and the Ugly. 2015. Available online: <https://nmr.physics.ox.ac.uk/teaching/wavecon.pdf> (accessed on 17 January 2022).
34. Blackledge, J.M.; Kearney, D.; Lamphiere, M.; Rani, R.; Walsh, P. Econophysics and Fractional Calculus: Einstein’s Evolution Equation, the Fractal Market Hypothesis, Trend Analysis and Future Price Prediction. *Mathematics* **2019**, *7*, 1057. [CrossRef]
35. Kolmogorov, A.N. On Analytic Methods in Probability Theory. *Math. Ann.* **1931**, *104*, 451–458.
36. Feller, W. On Boundaries and Lateral Conditions for the Kolmogorov Differential Equations. *Ann. Math.* **1957**, *65*, 527–570. [CrossRef]
37. Blackledge, J.M. Application of the Fractional Diffusion Equation for Predicting Market Behaviour. *Int. J. Appl. Math.* **2010**, *40*, 134–158. [CrossRef]
38. Blackledge, J.M.; Lamphiere, M. A Review of the Fractal Market Hypothesis for Trading and Market Price Prediction. *Mathematics* **2022**, *10*, 117. [CrossRef]
39. Blackledge, J.M. Diffusion and Fractional Diffusion Based Image Processing. In *EG UK Theory and Practice of Computer Graphic*; Tang, W., Collomosse, J., Eds.; The Eurographics Association: Geneva, Switzerland, 2009; pp. 233–240. [CrossRef]
40. Blackledge, J.M.; Blackledge, M.D. Fractional Anisotropic Diffusion for Noise Reduction in Magnetic Resonance Images. *ISAST Trans. Electron. Signal Process.* **2010**, *4*, 44–57. [CrossRef]

41. Blackledge, J.M.; Blackledge, M.D. Magnetic Resonance Image Processing Using Levy Distributed Anisotropic Diffusion. In Proceedings of the 10th International Conference on Environment and Electrical Engineering IEEEIC, Rome, Italy, 23–24 June 2011; pp. 1–7. Available online: <https://arrow.tudublin.ie/engscheleart/200/> (accessed on 30 January 2022).
42. Geim, A.K.; Novoselov, K.S. The Rise of Graphene. *Nat. Mater.* **2007**, *6*, 183–191. [CrossRef]
43. Novoselov, K.S.; Geim, A.K.; Morozov, S.V.; Jiang, D.; Katsnelson, M.I.; Grigorieva, I.; Dubonos, S.; Firsov, A. Two-dimensional Gas of Massless Dirac Fermions in Graphene. *Nature* **2005**, *438*, 197–200. [CrossRef]
44. Kim, P. Graphene and Relativistic Quantum Physics. 2015. Available online: <http://www.bourbaphy.fr/kim.pdf> (accessed on 13 January 2022).
45. Wikipedia. Green's Function. 2022. Available online: https://en.wikipedia.org/wiki/Green%27s_function (accessed on 4 February 2022).
46. Blackledge, J.M.; Babajanov, B. The Fractional Schrödinger-Klein-Gordon Equation and Intermediate Relativism. *Int. J. Pure Appl. Math.* **2013**, *3*, 601–615.
47. WolframAlpha. Convolution of Two Functions. 2022. Available online: <https://www.wolframalpha.com/input/?i=convolution+of+two+functions> (accessed on 25 January 2022).